Buffer layers and transparent conducting oxides for chalcopyrite Cu(In,Ga)(S,Se)2 based thin film photovoltaics: Present status and current developments

ARTICLE *in* PROGRESS IN PHOTOVOLTAICS RESEARCH AND APPLICATIONS · SEPTEMBER 2010

Impact Factor: 7.58 · DOI: 10.1002/pip.955 · Source: OAI

PROGRESS IN PHOTOVOLTAICS: RESEARCH AND APPLICATIONS
Prog. Photovolt: Res. Appl. 2010; **18**:411–433
Published online 15 April 2010 in Wiley Online Library (wileyonlinelibrary.com). DOI: 10.1002/pip.955

SPECIAL ISSUE PAPER

Buffer layers and transparent conducting oxides for chalcopyrite Cu(In,Ga)(S,Se)$_2$ based thin film photovoltaics: present status and current developments

N. Naghavi[1]*, D. Abou-Ras[2], N. Allsop[2], N. Barreau[3], S. Bücheler[4], A. Ennaoui[2], C.-H. Fischer[2], C. Guillen[5], D. Hariskos[6], J. Herrero[5], R. Klenk[2], K. Kushiya[7], D. Lincot[1], R. Menner[6], T. Nakada[8], C. Platzer-Björkman[9], S. Spiering[6], A.N. Tiwari[4] and T. Törndahl[9]

[1] Institut de Recherche et Développement sur l'Energie Photovoltaïque (IRDEP -UMR 7174 EDF-CNRS-ENSCP), 6 quai Watier, 78401 Chatou Cedex, France
[2] Helmholtz-Zentrum Berlin für Materialien und Energie GmbH, Solar Energy Division, Glienicker Strasse 100, 14109 Berlin, Germany
[3] Institut des Matériaux Jean Rouxel (IMN)-UMR 6502, Université de Nantes, CNRS, 2 rue de la Houssinière, BP 32229, 44322 Nantes Cedex 3, France
[4] Laboratory for Thin Films and Photovoltaics, Empa. Swiss Federal Laboratories for Materials Testing and Research, Ueberlandstr. 129, 8600 Duebendrof, Switzerland
[5] Departamento de Energía (CIEMAT), Avenida Complutense 22, Madrid 28040, Spain
[6] Zentrum für Sonnenenergie- und Wasserstoff-Forschung Baden-Württemberg, Industriestrasse 6, 70565 Stuttgart, Germany
[7] Showa Shell Sekiyu K.K. New Business Development (NBD) Div. CIS R&D Group, 123-1, Shimo-kawairi, Atsugi, Kanagawa, Japan
[8] Department of Electrical Engineering and Electronics, L-317 Aoyama Gakuin University, 5-10-1 Fuchinobe, Sagamihara, Kanagaw Pref. 229-8558, Japan
[9] Ångström Solar Center, Uppsala University, P.O. Box 534, SE-751 21 Uppsala, Sweden

ABSTRACT

The aim of the present contribution is to give a review on the recent work concerning Cd-free buffer and window layers in chalcopyrite solar cells using various deposition techniques as well as on their adaptation to chalcopyrite-type absorbers such as Cu(In,Ga)Se$_2$, CuInS$_2$, or Cu(In,Ga)(S,Se)$_2$. The corresponding solar-cell performances, the expected technological problems, and current attempts for their commercialization will be discussed. The most important deposition techniques developed in this paper are chemical bath deposition, atomic layer deposition, ILGAR deposition, evaporation, and spray deposition. These deposition methods were employed essentially for buffers based on the following three materials: In$_2$S$_3$, ZnS, Zn$_{1-x}$Mg$_x$O. Copyright © 2010 John Wiley & Sons, Ltd.

KEYWORDS

Cd-free buffer layers; window layers; transparent conducting oxides; chalcopyrite-based solar cells; Cu(In,Ga)(S,Se)$_2$

***Correspondence**

N. Naghavi, Institut de Recherche et Développement sur l'Energie Photovoltaïque (IRDEP -UMR 7174 EDF-CNRS-ENSCP), 6 quai Watier, 78401 Chatou Cedex, France.
E-mail: negar-naghavi@chimie-paristech.fr

Received 15 March 2009; Revised 11 November 2009

1. INTRODUCTION

The process technology of chalcopyrite-type thin-film solar cells based on Cu(In,Ga)Se$_2$ (CIGS) and related absorbers such as CuInS$_2$ (CIS) and Cu(In,Ga)(S,Se)$_2$ (CIGSSe), which in general consist of a glass/Mo/CIGS/CdS/i-ZnO/ZnO:Al stack, has reached maturity for mass production. At present, the highest efficiencies are obtained using CdS buffer layers deposited by chemical bath deposition (CBD) with a record conversion efficiency of 19·9% for a 0·5 cm^2 laboratory cells [1], 16·6% on 16 cm^2 mini-modules [2], and 13% on 60×120 cm^2 modules [3]. However, because of both environmental reasons and the fact that the common CdS layer with a

band-gap energy of about 2·4–2·5 eV limits the level of optimum performance of the cells, especially in the short wavelengths domain, one of the major objectives in the field of CIGS technology remains the development and implementation in the production line of Cd-free alternative buffer layers.

The development of Cd-free devices started in 1992 and intensively continued to the current efficiency level of 19% as shown in a very complete review paper in 2005 [4].

Among various materials and deposition methods which have been studied during the last decade, some of them have reached maturity and present potential for industrial applications. A general conclusion of the investigations during the last decade suggests that the most relevant materials are films based on In_2S_3, ZnS, $Zn_{1-x}Mg_xO$, and their derivatives using the following deposition techniques: chemical bath deposition (CBD), atomic layer deposition (ALD), ion-layer gas reaction (ILGAR), sputtering and evaporation (PVD), and ultrasonic spray pyrolysis (USP).

A major advantage of these alternative materials is that their band-gap energies are larger than that of CdS (except for indium sulfide, for which band-gap energies have been reported in a wide range between 2·0 and 2·8 eV). Therefore, the blue absorption losses in the buffer layer are reduced as compared with solar cells containing a CdS buffer. In_2S_3, ZnS, $Zn_{1-x}Mg_xO$ are n-type semiconductors and are thus suitable partners for the p-type chalcopyrite absorbers. However, for industrial applications, further important criteria must be taken into account:

- production costs (e.g., deposition time and waste management);
- technological feasibility (e.g., development of suitable large-area deposition systems);
- reproducibility and long-term device stability (e.g., effects of post-deposition treatments such as light soaking or annealing).

The aim of the present contribution is to give a review on the recent work performed since the reviews by Hariskos *et al* [4]. and Siebentritt [5], covering buffer and window-layer issues, various deposition techniques and their adaptation to the CIGS absorber, emphasis on solar-cell performances, the expected technological problems, and current attempts of their commercialization.

2. GENERAL ASPECTS

Given the complexity of the device it is quite remarkable that the standard chalcopyrite solar cell (soda lime glass, molybdenum back contact, absorber with a band gap of about 1·1 eV, CBD-CdS buffer layer, undoped ZnO, highly doped ZnO) is well behaved in the sense that it reaches high efficiency, has been prepared in different laboratories with similar properties, exhibits only mild meta-stability and shows no inherent degradation under many conditions (illumination, dry heat, radiation) and could be scaled to large areas. In state-of-the-art devices there is a clearly dominant recombination mechanism generating the bucking current which is essentially thermally activated with an energy corresponding to the absorber band gap. The collection of photogenerated carriers from the absorber is almost perfect while all carriers generated in the window are lost. On the other hand, modifications of the standard device quite often result in a weakening of these desirable properties. Obviously, the physics of the standard device are not understood well enough to carry out such modifications in a fully controlled fashion. Replacement of the standard CBD-CdS buffer layer by a different material (and in some cases using a different deposition technology) is a typical example.

In a chalcopyrite cell, the buffer establishes the interface properties, the undoped ZnO (i-ZnO) decouples poorly performing locations [6], the highly doped ZnO is responsible for lateral current transport. By using different materials for different functions they can be optimized separately (to a certain degree). In order to better understand the requirements for the alternative buffer layer one has to consider the basic requirements in terms of the electronic model of the device [7] and what makes CBD-CdS an exceptional material in this context. The most important requirements are:

- a sufficiently wide band gap (low optical absorption);
- a suitable conduction band line-up to the absorber and to the undoped ZnO;
- a very low defect density at the absorber/buffer interface; and/or
- position of the Fermi level at the absorber/buffer interface close to the absorber conduction band (energetically shallow donor-type interface defects), i.e., complete inversion of the absorber surface.

According to literature data the first two requirements are fulfilled more or less by the CBD-CdS and it is not too difficult to find alternative materials than can do so likewise. We therefore assume that the latter two requirements are much harder to satisfy. The CdS may have an advantage over other materials due to lattice matching as indicated by low temperature epitaxial growth under some conditions reported in the literature [8]. However, given typical process conditions, it is reasonable to assume that there is always a significant density of interface defects. Also, CdS buffers perform comparatively well on absorbers with different lattice constants. We may therefore speculate that the combination of a chalcopyrite surface and a CBD-CdS buffer is exceptional because the Fermi-level position at the interface is very well defined. It is well known that the surface of polycrystalline chalcopyrite films is deficient in copper [9]. It has also been reported that Cd moves into the absorber surface [10]. We may speculate that Cd-doping works effectively in this copper-deficient material [11]. It is, however, not exactly clear how far the copper deficiency extends into the absorber. The idealized boundary cases are a surface reconstruction [12,13] or the surface segregation of a distinct Cu-deficient phase [14]. In the former case the

DOI: 10.1002/pip.955

electrostatic charge is essentially concentrated in a plane. The shallow donor would be positively charged Cd occupying sites with a particular bonding situation (at the transition from the reconstructed absorber surface to the CdS lattice). This could explain why an actual CdS film yields better results than attempts to merely dope the surface with Cd. In the case of a Cu-deficient surface segregation we might form a buried junction [15]. This is undesirable because it reduces the blue response of the junction. On the other hand, the segregated phase may have a wider band gap than the bulk absorber which would limit the optical absorption and corresponding losses in blue response (it acts like a built-in buffer layer).

In summary, while there are many unresolved questions, it is a plausible speculation that Cd forms a beneficial stable donor-type defect in Cu-deficient surfaces of chalcopyrite thin films, in a suitable concentration and at a suitable energetic position in the gap. The wet chemical process may assist this junction formation by its *in situ* cleaning effect which minimizes the formation of harmful defects (e.g., related to oxygen). The challenge in developing an alternative buffer lies in establishing a similarly effective defect chemistry, resulting in an appropriate charge density and ultimate Fermi-level position at the interface. Results suggest that with many alternative buffer layers one has to rely on post-deposition annealing or photodoping (light soaking) to establish the charge density. Even then, good performance is sometimes only achieved with certain types of absorbers.

Tables I and II summarize the best Cu-chalcopyrite-based solar-cell efficiencies reported (cell area $\leq 1\,cm^2$) and modules produced with various zinc- and indium-based buffer layer materials deposited by various methods. When analyzing these results, it has to be kept in mind that the quality and composition of the absorbers may vary significantly between the production runs and laboratories. In order to evaluate the quality of the Cd-free junction formation, the performance of the best devices was compared with reference devices containing CBD-CdS.

For most of these buffers, no matter which deposition technique, the replacement of CdS improves essentially the J_{sc} of cells, an effect which can be attributed to the higher band-gap energy of these buffers compared to CdS (Table I).

A comparison of the efficiencies of cells shows that for most deposition techniques it is possible to reach Cd-free cells exhibiting conversion efficiencies equivalent or higher than the corresponding CdS reference cells (Figure 1).

However, based on results presented in Figure 2, some highly efficient Cd-free modules are obtained, even though some progress in terms of stability and reproducibility is necessary. As shown in the next sections, the lower conversion efficiencies of Cd-free modules seem to be caused either by technological up-scaling problems or the need for special post-treatments of these modules.

In the following sections, we give more detailed descriptions of the different material systems and techniques most studied during the last decade. However, some new and promising techniques have emerged and been studied lately such as electrodeposition (ED) leading to a maximum photoelectric conversion efficiency of 7·1% on $CuInS_2$ limited mainly by a low fill factor (FF, 51%) [16]. Metal-organic chemical-vapor deposition (MOCVD) of In_2S_3, is another promising technique leading to an efficiency of 12·3% (CdS reference = 13·0%) on CIGS [17]. Further process optimization is expected for both techniques to lead to efficiencies comparable to CdS buffers [16,17].

3. CHEMICAL BATH DEPOSITION

CBD is the method most frequently applied for the deposition of CdS buffer layers. The highest and most reproducible solar-cell efficiencies, independent of the absorber used, are obtained by use of the classical CBD-CdS/i-ZnO layer stack. It has been suggested not only that buffer layers deposited by the CBD process function as a protection of the pn-junction from plasma damage during subsequent ZnO sputtering and prevent undesirable shunt paths, but also that chemically deposited buffer layers permit a conformal and pinhole-free coating of the absorber by the CdS layer. Moreover, when the glass/Mo/absorbers stack is immersed into the chemical bath for the buffer deposition, the CIGS layer surface is probably also subjected to beneficial chemical etching of the surface, e.g., the ammonia used in most CBD recipes is thought to be crucial for the cleaning of absorber surface by removal of oxides and other impurities [18]. In addition, n-type doping of the CIGS region close to the surface by Cd or Zn from the CBD solution has been reported [19,20].

CBD involves the precipitation from the solution of a compound on a suitable substrate. This method offers many advantages such as control of film thickness and deposition rate by varying the solution pH, temperature, and reagents concentration allied with the ability of CBD to coat large areas by a reproducible low cost process. However, the CBD of sulfides usually results in films containing hydroxides and/or oxides. Therefore, CBD films are often described in the literature as $M_x(S,O,OH)_y$ or $M_xS_y(O,OH)$, etc. (M = Cd, Zn, In, etc.). The unsatisfying controllability of the composition of these films and the generation of a substantial quantity of liquid wastes remain the most important disadvantages of the CBD.

3.1. ZnS-based buffer layer

The CBD-ZnS remains one of the most studied Cd-free buffer layer for replacing CBD-CdS. The development of the CBD-ZnS buffer started in the beginning of the 1990s [21,22]. However, the most important progress has been made during the past decade initiated by Showa Shell [23]. Since then new bath compositions have been developed, all of them leading to very high efficiencies compared to their

Table I. Summary of the best Cd-free chalcopyrite based solar cells compared to their CdS references.

Deposition methods	Buffer layer	Absorber	Window layers	Efficiency (%)	V_{oc} (V)	J_{sc} (mA/cm^2)	FF (%)	Area (cm^2)	References
	Zn(S,O)	$CuInS_2$		10·4	0·700	22·5	65·8	0·5	[29]
	ref. CdS		r.f. i-ZnO/ZnO:Al	**10·3**	**0·700**	**21·4**	**68·0**	**0·5**	
	Zn(S,O)	$Cu(In,Ga)(S,Se)_2$		14·9	0·560	39·0	68·3	0·5	[31]
	Zn(S,O,OH)	$Cu(In,Ga)Se_2$	r.f. ZnO:Al	18·5	0·669	35·1	78·8	0·402	[27]
	ref. CdS			**17·2**	**0·648**	**35·0**	**76·2**	0·402	
	Zn(S,O,OH)	$Cu(In,Ga)Se_2$	r.f. $Zn_{1-x}Mg_xO$/ZnO:Al	18·0[a]	0·68	34·5	77·0	0·5	
CBD	**ref. CdS**		**r.f. i-ZnO/ZnO:Al**	**16·2**	**0·682**	**31·0**	**76·7**	**0·5**	[33]
	Zn(S,O,OH)	ED-$CuIn(S,Se)_2$	r.f. $Zn_{1-x}Mg_xO$/ZnO:Al	8·1	0·705	19·2	60·0	0·5	
	ref. CdS		**r.f. i-ZnO/ZnO:Al**	**8·0**	**0·750**	**16·8**	**61·0**	**0·5**	[35]
	Zn(S,O,OH)	$CuGaSe_2$	r.f. $Zn_{1-x}Mg_xO$/ZnO:Al	5·3	0·773	13·1	52·0	0·5	
	ref. CdS		**r.f. i-ZnO/ZnO:Al**	**4·2**	**0·841**	**10·0**	**50·0**	**0·5**	[36]
	InS_xO_y	$CuInS_2$	r.f. i-ZnO/ZnO:Al	8·8	0·700	21·6	56·0	0·5	
	ref. CdS			**9·9**	**0·706**	**21·0**	**66·0**	**0·5**	[45]
	In_2S_3 spray-ILGAR			14·7	0·574	37·4	68·4	0·5	
	ref. CdS			**13·9**	**0·580**	**39·6**	**60·3**	**0·5**	[53]
	ZnS:In_2S_3 spray-ILGAR	$Cu(In,Ga)(S,Se)_2$	r.f. i-ZnO/ZnO:Al	15·3	0·580	38·8	68·0	0·5	[56]
	Cd^{2+} treated absorber/ZnO dip			15·0	0·580	35·1	73·7	0·5	
ILGAR	ILGAR								[51]
	ref. CdS			**14·1**	**0·588**	**32·9**	**73·1**	**0·5**	
	Cd^{2+} treated absorber/ZnO dip-ILGAR	$Cu(In,Ga)(S,Se)_2$	r.f. ZnO:Ga	14·5	0·575	34·9	71·4	0·5	
	ref. CdS			**14·7**	**0·597**	**34·0**	**72·3**	**0·5**	[50]
	In_2S_3 co-evaporation			13·3	0·606	29·6	74·0	0·5	
PVD	**ref. CdS**			**14·0**	**0·610**	**31·4**	**73·0**	**0·5**	[65]
	In_2S_3 compound evaporation	$Cu(In,Ga)Se_2$	r.f. i-ZnO/ZnO:Al	15·2	0·677	29·8	75·6	0·528	
	ref. CdS			**16·3**	**0·651**	**32·8**	**76·4**	**0·5**	[66]
	In_xS_y reactive			11·1	0·652	24·7	69·1	0·5	[72]
	In_xS_y ceramic	$Cu(In,Ga)Se_2$	**r.f. i-ZnO/ZnO:Al**	13·3	0·637	28·8	72·3	0·5	[73]
	ref. CdS			**14·4**	**0·668**	**28·4**	**76·1**	**0·5**	

DOI: 10.1002/pip.955

Sputtering	$Zn_{1-x}Mg_xO$	$Cu(In,Ga)(S,Se)_2$	$Zn_{0.85}Mg_{0.15}O/ZnO:Al$	13·1	0·543	36·9	65·5	0·5	
	ref. CdS		**r.f. i-ZnO/ZnO:Al**	**14·3**	**0·586**	**34·1**	**71·7**	**0·5**	[79]
	$Zn_{1-x}Mg_xO$	$CuInS_2$	$Zn_{0.85}Mg_{0.15}O/ZnO:Al$	8·2	0·648	20·5	61·7	0·5	
	ref. CdS		**$Zn_{0.85}Mg_{0.15}O$/ZnO:Al**	**9·4**	**0·670**	**20·3**	**68·9**	**0·5**	[81]
	In_2S_3			16·4	0·665	31·5	78·0	0·1	[88]
ALD	Zn(O,S)	$Cu(In,Ga)Se_2$	r.f. i-ZnO/ZnO:Al	18·5[a]	0·689	35·5	75·8	0·5	[85]
	$Zn_{1-x}Mg_xO$			18·1[a]	0·668	35·7	75·7	0·5	
	ref. CdS			**16·7**	**0·671**	**32·8**	**75·8**	**0·5**	[87]
	In_2S_3	$Cu(In,Ga)(S,Se)_2$		12·4	0·502	34·7	71·0	0·3	
USP	**Ref. CdS**		r.f i ZnO/ZnO:A1	**10·5**	**0·521**	**31·1**	**65·0**	**0·3**	[63]
	In_2S_3	$Cu(In,Ga)Se_2$		11·9	0·543	30·2	73·0	0·3	
	ref. CdS			**12·5**	**0·570**	**30·3**	**73·0**	**0·3**	This paper

[a] With MgF_2 ARC.

Table II. Summary of the best Cd-free chalcopyrite-based solar modules.

Deposition methods	Buffer layer	Absorber	Window layers	Efficiency (%)	V_{oc} (V/cell)	J_{sc} (mA/cm^2)	FF (%)	Area (cm^2)	References
CBD	Zn(S,O)	$CuInS_2$	r.f. i-ZnO/ZnO:Al	7·1	0·650	18·5	59·4	100	
				6·6	0·680	19·5	50·4	900	[31]
	ref. CdS			**7·8**	**0·660**	**19·1**	**64·0**	**900**	
	Zn(S,O)	$Cu(In,Ga)(S,Se)_2$	r.f. i-ZnO/ZnO:Al	12·4	0·540	34·3	67·8	100	
				12·5	0·550	34·5	65·5	900	[31]
	ref. CdS			**12·5**	**0·550**	**33·7**	**66·8**	**900**	
	Zn(S,O,OH)	$Cu(InGa)Se_2$	r.f. $Zn_{1-x}Mg_xO/ZnO:Al$	15·2	0·667	72·0	72·0	62·7	[33]
	Zn(S,O,OH)	$Cu(InGa)(S,Se)_2$ surface layer/$Cu(InGa)Se_2$ absorber	MOCVD ZnO:B	15·2	0·601	36·18	70·0	855	[48]
ILGAR	In_2S_3	$Cu(In,Ga)(S,Se)_2$	r.f. i-ZnO/ZnO:Al	12·4	0·534	34·4	67·5	100	This paper
Sputtering	In_xS_y ceramic	$Cu(InGa)Se_2$	r.f. i-ZnO/ZnO:Al	11·2	0·632	63·6	27·9	48	[73]
ALD	In_2S_3	$Cu(In,Ga)Se_2$	r.f. i-ZnO/ZnO:Al	12·9	0·662	27·8	72·6	714	
	ref. CdS			**12·9**	**0·657**	**27·6**	**71·5**	**714**	[89]
	Zn(O,S)	$Cu(In,Ga)Se_2$	r.f. i-ZnO/ZnO:Al	12·7	0·648	29·0	67·4	724	[86]
	Zn(O,S)			14·7	0·685	30·7	70·3	77	[84]
	ref. CdS			**13·3**	**0·614**	**30·9**	**69·9**	**77**	

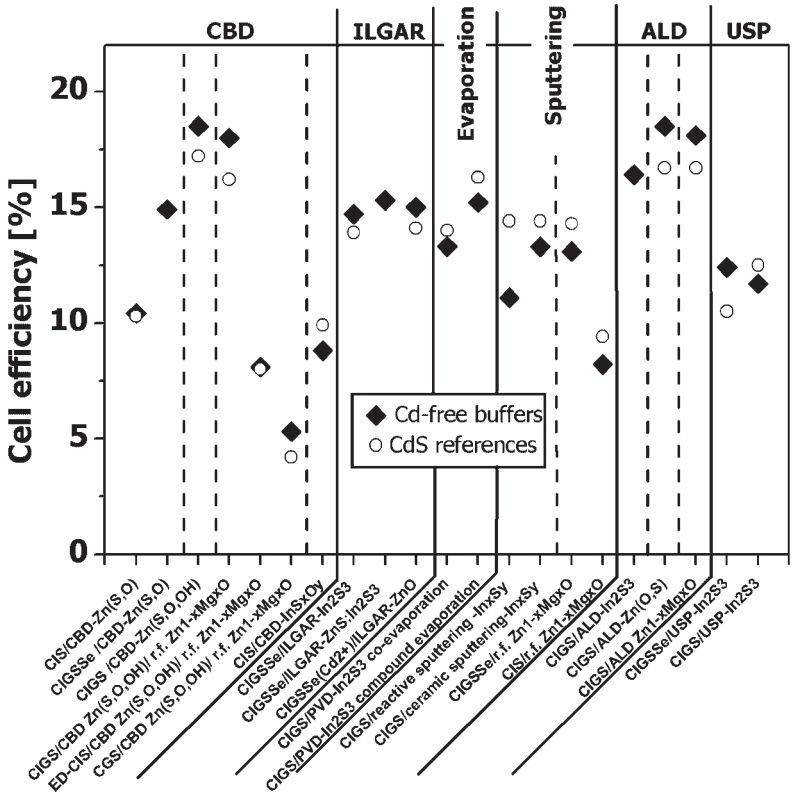

Figure 1. Summary of the best chalcopyrite-based solar-cells efficiencies ($A \leq 1\,cm^2$) realized with different Cd-free buffer layer materials and deposited by different methods compared to their reference devices containing CBD-CdS.

CdS references [24–27]. Depending on the deposition conditions, usually a composition of the type Zn(S,O,OH) is easily obtained, thus the layer is a mixture of ZnS, ZnO, and $Zn(OH)_2$. The CBD-ZnS films have often been synthesized in basic medium using a zinc salt, with thiourea as sulfur precursor and ammonia as complexing agent. In the first CBD-ZnS deposition buffers leading to conversion efficiencies of about 12%, highly toxic reactants such as hydrazine were applied as additional complex agent in order to increase the growth rate. However, the bath compositions more recently reported avoid the use of this toxic reactant.

The two first CBD-ZnS recipes providing reduced toxicity were developed first at Showa Shell Sekiyu, with solar-cell efficiencies of 14–15% on $100\,cm^2$-sized substrates, and then by Nakada and Contreras on a world record absorber leading to the record conversion efficiency of 18·6% [25,27]. The most important differences between these processes were the absorber used as observed in Figure 3, and the ammonia concentration used for the CBD bath. Nakada and Mizutani [25] used a bath composed of $ZnSO_4$ (0·16 M)-ammonia (7·5 M)-thiourea (0·6 M) aqueous solution at 80°C. Thick films (100 nm) for solar cells were obtained by repeating this CBD process about 3 times for 15 min. These Zn(S,O,OH) layers consisted of nanoparticles with a large amount of oxygen included in the form of $Zn(OH)_2$ and ZnO in the ZnS layer. The [S]/([S] + [O]) ratio decreased toward the CIGS absorber layer, suggesting a decrease of band-gap energy [28]. The optical band-gap energy was determined to be 3·7 eV from transmission and reflection measurements.

Ennaoui *et al* [29]. developed a novel chemical routes based on two Zn complexes: $[Zn(SC(NH_2)_2)_n]^{2+}$ and $[Zn(NH_3)_n]^{+2}$ for industrial $CuInS_2$ (CIS) and Cu(In, Ga)(S,Se)$_2$ (CIGSSe) absorbers (Figure 3). Samples buffered at the optimum conditions ($T = 75°C$, $[ZnSO_4] = 0{\cdot}15$ mol/L, $[SC(NH_2)_2] = 0{\cdot}60$ mol/L, $[NH_3] = 30\%$) and completed with i-ZnO/ZnO:Al windows exhibit total-area ($0{\cdot}5\,cm^2$) efficiencies of up to 14·9% for Cu(In,Ga)(S,Se)$_2$ (CIGSSe) and 10% for $CuInS_2$ (CIS) which is 10% higher than their CdS references [29–31].

In general the high efficiency of ZnS/i-ZnO layers are obtained after a post-deposition annealing and/or photo-doping (light soaking). In order to reduce/suppress these post-treatments and improve the stability of these cells, recently studies on the combination of ZnS/ $Zn_{1-x}Mg_xO$ layers as replacement for the CdS/i-ZnO stack have been performed [32–36]. The Zn(S,O,OH)/$Zn_{1-x}Mg_xO$ buffer combination was used for the first time by Minemoto *et al*. [37] in the device structure ITO/$Zn_{1-x}Mg_xO$/Zn(S,O,OH)/CIGS/Mo/glass. The CIGS films were first dipped in a $Cd^{2+}_{(aq)}$ solution in order to form a buried junction and the Zn(S,O,OH) buffer layer were deposited by CBD with a few nanometers thickness. The $Zn_{1-x}Mg_xO$ layers were

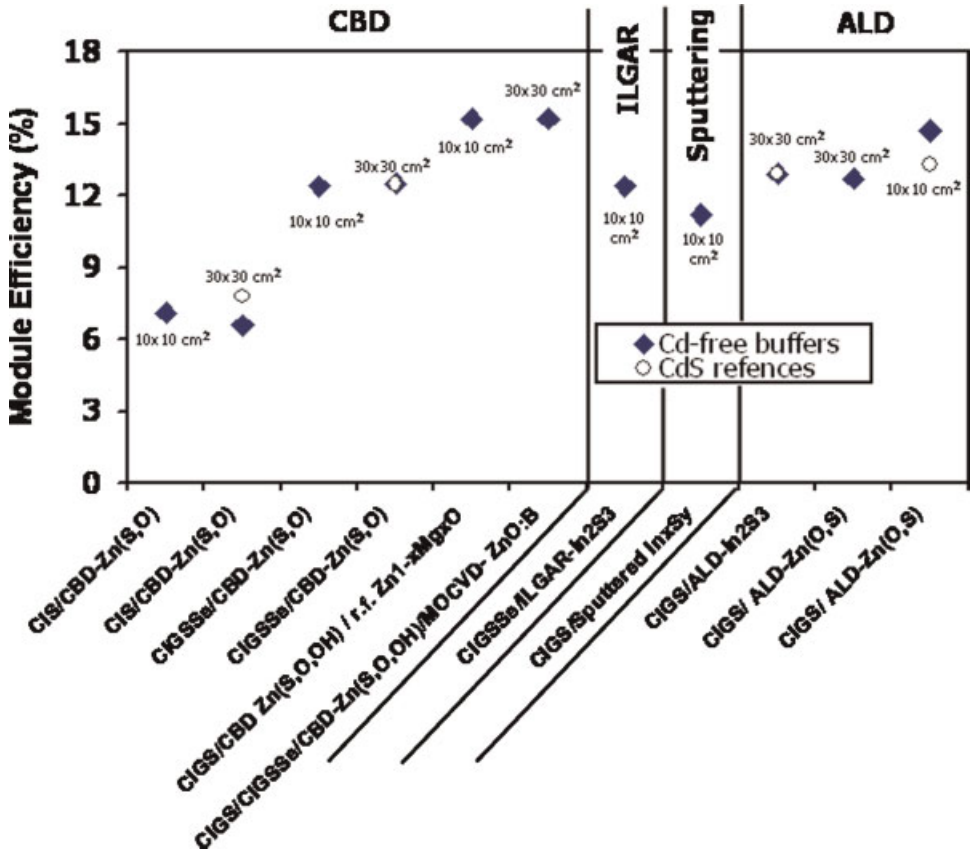

Figure 2. Summary of the best chalcopyrite-based solar modules efficiencies realized with different Cd-free buffer layer materials and deposited by different methods compared to their reference devices containing CBD-CdS.

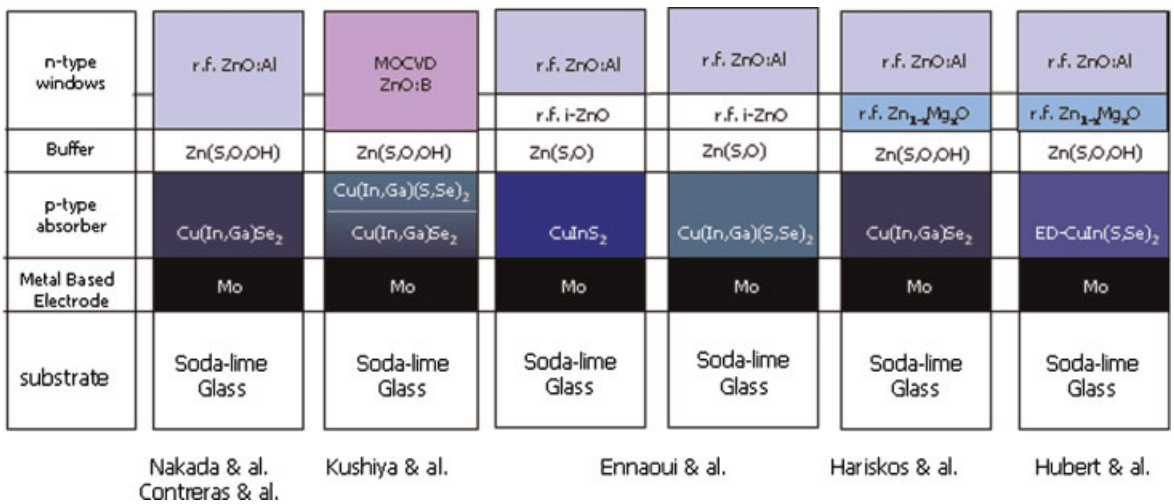

Figure 3. Device structure of chalcopyrite-based solar devices using CBD-ZnS-based buffer layers.

prepared by r.f. co-sputtering from ZnO and MgO targets. The conduction band off-set was adjusted by changing the Mg content x. In recent studies Zn(S,O,OH)/$Zn_{1-x}Mg_xO$ buffer combinations have been used on in-line co-evaporated CIGS [32,33], $CuGaSe_2$ [36], and electro-deposited CIGSSe [34,35] absorbers. The deposition of the CBD-Zn(S,O,OH) was carried out at similar conditions as the conventional CdS buffer from a $ZnSO_4$, ammonia, and

thiourea solution at temperatures of about 80°C with thicknesses between 20 and 40 nm, and aiming at a reduction of deposition time below 10 min [32–35]. The growth mechanisms leading to different film compositions were investigated on the basis of theoretical solution chemistry considerations. These studies showed that the deposition mechanisms seem to be surface reactions with low dependence on the hydrodynamic regimes. Moreover, for this condition, in the first stage of deposition it is not possible to avoid the presence of ZnO and $Zn(OH)_2$ in the films [34,35]. The $Zn_{1-x}Mg_xO$ layer was r.f. sputtered from different ceramic $Zn_{1-x}Mg_xO$ targets with a defined composition. Highly efficient ZnO:Al/$Zn_{1-x}Mg_xO$/Zn(S,O,OH)/CIGSe devices with up to 18% efficiency with improved stability were demonstrated. Cells with the new buffer concept show higher conversion efficiencies than with the traditional CBD-CdS.

3.2. In_2S_3-based buffer layer

The record efficiency with CBD-In_2S_3 was obtained in 1996 [38]. Since then, efforts were directed to a better understanding of growth mechanisms. Based on theoretical and experimental studies, it has been shown that the formation of In_2S_3 is easier in acidic medium. Usually in CBD-In_2S_3, the thiourea is replaced by thioacetamide (TA) mainly because of its higher decomposition in acidic medium. The growth of thin films from aqueous In(III) and TA solutions consists of the parallel deposition of indium sulfide, indium hydroxide, and indium oxide that compete under different experimental conditions such as solution composition, temperature, or reaction time [39–42]. Based on these studies, it has been shown that the deposition of In_2O_3 is favored at low bath temperature, at low TA concentration, and at the beginning of the reaction time, probably resulting in films with higher oxide proportion. Besides, additives like acetic acid and hydrochloric acid can also control the incorporation of indium hydroxide and/or oxide to the layer deposited. Thin films with compositions in the range of [S]/[In] = 0·6–1·3 have been obtained [43], with corresponding band-gap energies ranging between 2·0 and 3·6 eV, and resistivity values from 10^7 to $10^8\,\Omega$ cm [39,41]. Thus, it is possible to tune chemical and physical properties of CBD-In_2S_3 films (mainly composition, transparency, and absorption edge) from values near that of In_2S_3 to that of In_2O_3. The highest efficiency values on $CuInS_2$ absorbers of 8·8% have been reached with buffers deposited at relatively high temperature of 70°C and TA concentration of 0·3 M, adding acetic acid (0·3 M) and hydrochloric acid (0·01 M) leading to a short induction time (5 min) and high deposition rate (30 nm/min) [44,45]. However, for these films, light soaking is needed in order to improve the V_{oc} and efficiency of the corresponding devices, especially for the buffer with a higher In_2S_3 content.

More recently, deposition of buffers from the same CBD formulation with mixed ions (In^{3+}/Zn^{2+}) has resulted in the production of devices with improved open-circuit voltage and conversion efficiency [46], by using ammonia-free solutions and allowing for a reduction of the indium consumption. However, more efforts are needed in order to improve the efficiency of CBD-In_2S_3-based cells and to minimize the post-treatment effects.

3.3. Up-scaling and outlook

For CBD-In_2S_3, the first up-scaling studies have shown that it is possible to prepare large-area samples up to $15 \times 30\,cm^2$ substrates, exhibiting good homogeneities and optical transmittance variations below 2% (over 95% of the surface) [47]. In order to allow a scalable process, recycling and minimization of wastes are required. Indium metal recovery has already been implemented by electro-winning with the possibility to recover more than 99% of indium with 99·98% purity. Moreover, Honda Soltec in Japan seems to have successfully introduced CBD-In_2S_3 ($In(S,OH)_x$) process into their production line.

The CBD-ZnS has been transferred successfully to a 20 MW/a CIS production plant of Showa Shell Sekiyu, suitable for 7200 cm^2 substrates. A 60 MW/a production line with CBD-Zn(S,O,OH) buffer deposition was also initiated. A careful adjustment of the thickness of the Zn(S,O,OH) buffer layer in the combination with a ZnO:B (BZO) window prepared by an MOCVD technique has led to an FF of more than 0·7 for thin-film circuits on a 900 cm^2 sized substrate. These results have so far been obtained using a $Cu(InGa)(S,Se)_2$ surface layer/$Cu(InGa)Se_2$ absorber fabricated by sulfurization after selenization (SAS) method (Figure 3) [48].

Significant progress in the fabrication of high efficiency modules was also achieved by Ennaoui *et al*. by combining *in situ* turbidity measurement and surface analysis. It has been showed that the oxygen concentration present in the buffer can be varied and the deposition rate can be enhanced by using additives leading to achieve optimum conditions for a scalable CBD-Zn(S,O,OH) process with reduced deposition time. Samples produced yields for reproducible large-area ($30 \times 30\,cm^2$) conversion efficiencies of above 12% for CIGSSe and of above 7% on $10 \times 10\,cm^2$ for CIS absorbers, thus, reaching values close to 90% of the efficiencies of CdS-buffered reference cells [31].

The combination of CBD-Zn(S,O,OH)/$Zn_{1-x}Mg_xO$ has led to $10 \times 10\,cm^2$ modules with efficiencies higher than 15% using co-evaporated CIGS absorbers with low transient effects [34].

However, high efficiency of CBD-Zn(S,O,OH) modules are obtained generally after a post-deposition annealing and light soaking, which means that there should be a greater focus on a better understanding of these post-treatments in order to avoid them for industrial applications.

Finally, while the material cost of CBD-Zn(S,O,OH) seems to be sufficiently low, the waste disposal of the CBD solution may affect substantially the total cost of the buffer deposition.

DOI: 10.1002/pip.955

4. ILGAR

ILGAR is an alternative chemical method for the deposition of thin semiconductor layers, developed and patented by Fischer *et al* [49]. In this sequential, cyclic process, first a solution of a precursor compound is applied to a substrate by dipping or spraying, then a reactant gas, H_2S for metal sulfides or NH_3/H_2O for hydroxides/oxides is led over the solid precursor film, which is converted into the final product. These two steps are repeated until the desired layer thickness is obtained.

Initial work on buffer layers focused on the replacement of the CdS buffer with a Cd-partial electrolyte treatment of the absorber and a dip-ILGAR i-ZnO layer. Cells were completed either with a conventional sputtered ZnO bilayer window or just with the n-ZnO:Ga window. Efficiencies reached 15% roughly comparable to the CdS reference with industrial $Cu(In,Ga)(S,Se)_2$ absorbers [50,51].

4.1. In_2S_3-based buffer layer

Recent work focused on In_2S_3-based buffers produced by Spray-ILGAR. The process involves the generation of an $InCl_3$/alcohol aerosol by an ultrasonic or pressure nebulizer which is carried over the heated substrate at 200–250°C by a N_2 stream (Figure 4). An aerosol assisted CVD-like reaction forms the In(Cl,O,OH) precursor film which is subsequently converted into In_2S_3 by the H_2S gas [52]. This cycle is repeated 3–6 times. The resulting layers are conformal to the substrate. Using industrial $Cu(In,Ga)(S,Se)_2$ absorbers, a statistical comparison of the In_2S_3 buffer layers with the standard CBD-CdS buffers was made. The resulting efficiencies were absolutely comparable as was the stability in accelerated aging tests [53,54]. For the In_2S_3 buffer, an efficiency of 14·7% has been certified. No pre-treatments or pre-cleaning steps were used and the resulting cells do not require post-annealing or light soaking. Equally important is the broad range of buffer thickness and deposition temperature which results in efficient solar cells, showing that the process is very robust [53].

It is notable that the ILGAR indium sulfide layer contains significant amounts of Cl from the precursor and Cu and Na, as a result of diffusion from the absorber [55]. The exact role of the Cl needs to be investigated, but it seems not to be essential for the device performance.

Several possibilities to control the composition are available. Firstly by the process temperature, in the spray process, the residual chlorine content in the layer is a function of both the temperature and the H_2S gassing time. The second possibility of controlling the composition is to use the cyclical nature of the ILGAR process in order to change the material deposited and fabricate a nanostructured or multilayered buffer layer. In this way $ZnS:In_2S_3$ buffer layers were produced, which result in a small but reproducible increase in open-circuit voltage and device efficiency, compared to the pure-In_2S_3-buffered cells [56]. A cell efficiency of 15·3% was measured, and the voltage performance of the cell was correlated to the photoluminescence intensity of the absorber [57].

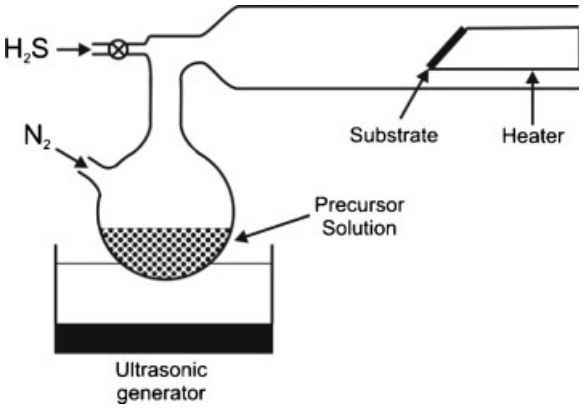

Figure 4. A schematic of the Spray-ILGAR equipment setup [52].

4.2. Up-scaling and outlook

Up-scaling to a $10 \times 10\,cm^2$ substrate size was developed in order to demonstrate the performance of the Spray-ILGAR In_2S_3 buffer on mini-modules. Heated absorber substrates were moved over a linear spray nozzle [58]. Modules based on $Cu(In,Ga)(S,Se)_2$ absorbers reached an efficiency of 12·4%. Further development of the fully in-line process to a moving 10 cm band has shown that the deposition efficiency with respect to indium consumption can be increased to over 30%, with further improvements expected. Experiments regarding the rate of deposition are currently under way with the goal of operating in excess of 1 m/min.

At CIS-Solartechnik, a roll-to-roll pilot-line including a fully in-line ILGAR machine is currently operating. Further production equipment for the industry is presently under development in an HZB cooperation with Stangl Semiconductor Equipment.

5. SPRAY PYROLYSIS

Spray pyrolysis is a low cost, large-area scalable, non-vacuum thin-film deposition technique which was first described by Chamberlin and Skarman [59]. With this method, a layer is formed on a heated substrate through a chemical reaction of thermally decomposed precursors. The reactants, delivered to the heated substrate surface, are dissolved in a solution which is nebulized to small droplet of micron-size range. The droplets are either generated by a pneumatic nozzle (high droplet velocity and broad distribution in droplet size) or by an ultrasonic actuator (low velocity and narrow distribution of droplet size) [60]. Spray pyrolysis has been used by several researchers to

grow metal-oxide, -sulfide, selenide layers for different components of solar cells.

5.1. In_2S_3 buffer layer

In_2S_3 by spray pyrolysis was first investigated by Kim and Kim [61] using a water–methanol-based solution with $InCl_3$ and $CS(NH_2)_2$ (thiourea) as precursors. They found that the metal to sulfur ratio in the precursor solution and the substrate surface temperature are the most important parameters for the In_2S_3 layer properties. For development of high efficiency CIGS cells the buffer layer should be deposited at low enough temperature to prevent surface oxidation of the absorber while maintaining required optical, electrical, and structural properties. Conditions need to be optimized to avoid detrimental impurities (elemental or compounds). Total-area efficiency of 8·9% with a glass/Mo/Cu(In,Ga)Se_2/In_2S_3/i-ZnO/ZnO:Al cell structure was reported by Ernits *et al*. [62] and an increase of the efficiency to 9·5% was observed due to continuous light soaking for 14 h at 80°C and 1 sun. An ultrasonic actuator was used to nebulize $InCl_3$ and thiourea dissolved in methanol ([In]/[S] = 1/3) and the layers were deposited at 380°C heater temperature. With the same method but using [In]/[S] = 1/4 and 200°C substrate surface temperature, total-area efficiency of 12·4% was obtained with a Cu(In,Ga)$(S,Se)_2$ absorber [63] and no light-soaking effects were observed. It was also shown that homogeneous polycrystalline In_2S_3 layers with low impurity concentration can be obtained at 200°C substrate surface temperature if sulfur is provided in excess.

To overcome possible surface oxidations of the absorber during the heating-up phase, the addition of citric acid as a reducing agent was recently introduced. With 0·002 mol/L citric acid, 0·02 mol/L $InCl_3$, and 0·03 mol/L thiourea dissolved in acetone and sprayed at 210°C substrate surface temperature on a Cu(In,Ga)Se_2 absorber 11·9% total-area efficiency was obtained after air annealing of the completed device at 200°C for 5 min. No significant light-soaking effects were observed.

The PV performance of CIGS-based solar cells with sprayed In_2S_3 buffer layer is significantly influenced by the absorber surface chemistry. With a Cu(In,Ga)Se_2 absorber by co-evaporation in a three-stage process, the best cell results so far were obtained with [Ga]/[Ga + In] = 0·18 in bulk of the absorber and a strong Ga grading in the third stage.

The spray pyrolysis technique is capable of in-line production with high throughput, it is a robust process and easy to control, it can be easily up-scaled [64], and the method is already widely used in the industry.

6. PHYSICAL VAPOR DEPOSITION

The advantages of these techniques (sputtering and evaporation) are that they are vacuum processes, which can be incorporated in-line with other vacuum processing steps and do not impact any liquid wastes. The main drawback with vacuum evaporation is poor contiguous coating of the CIGS films. Sputter deposition leads to more conformal coverage. The general success of sputtering for industrial large-area deposition motivated the exploration of sputter-deposited buffer layers.

6.1. In_2S_3 by evaporation

The deposition of both the chalcopyrite absorber and the buffer layer following a vacuum process should offer the possibility of an entire vacuum process line between patterning 1 (i.e., P1: Mo-scribe) and patterning 2 (i.e., P2: Cu(In,Ga)$(S,Se)_2$/buffer/r-ZnO scribe). It has been demonstrated during the last decade that Cu(In,Ga)Se_2 solar cells buffered with In_2S_3 grown by evaporation can reach performances close to those of a Cu(In,Ga)Se_2/CBD-CdS reference cells [64–70]. Record efficiencies of 15·2% on Cu(In,Ga)Se_2/evaporated-In_2S_3/ZnO structure has been recently obtained [66]. For this record efficiency cell, the buffer layer has been grown from the evaporation of In_2S_3 powder. This single source approach presents the advantage of avoiding the evaporation of elemental sulfur, which can be problematic for industrial implementation. The critical issue of this process is that the quality of the In_2S_3 powder can vary over the long deposition duration. This affects both the performance of the cells and the stability of the process [66–68]. The other possibility to deposit In_2S_3 by evaporation is the co-evaporation of elemental indium and sulfur, which also yields high efficiency devices [65]. This process is less dependent on the source materials and the sulfur evaporation issue mentioned above could be bypassed by a sequential evaporation approach instead of a simultaneous one [69]. Independently from the process, the best efficiencies are achieved when the In_2S_3 deposition is performed at low substrate temperatures (<100°C) and after annealing the complete device at 200–220°C in air for at least 15 min [65–70]. The origin of the performance improvement after post-annealing is still not well understood although it has been shown that it influences the Cu/In interdiffusions as well as the presence of Na at the Cu(In,Ga)Se_2/evaporated-In_2S_3 interface [65,71].

All of the investigations addressed for these devices lead to the conclusion that the junction quality, thus the cell efficiencies, are strongly dependent on interfacial diffusion mechanisms occurring during the In_2S_3 deposition and/or post-fabrication annealing. Consequently, the absorber (sub-)surface properties can be assumed of major importance for the cell operation.

6.2. In_2S_3 by sputtering

Magnetron sputtered indium sulfide layers as buffer for Cu(In,Ga)Se_2 (CIGS)-based solar cells were investigated

DOI: 10.1002/pip.955

by Hariskos *et al*. [72,73]. The material was deposited by (a) reactive sputtering from a metallic indium target, in a defined Ar/H_2S gas atmosphere with d.c. or r.f. plasma excitation and (b) r.f. sputtering from a stoichiometric ceramic indium sulfide target in pure Ar gas at power densities in the range of $1\,W/cm^2$. Small laboratory cells and mini-modules were realized with the device structure $CIGS/In_xS_y$/i-ZnO/ZnO:Al. For the deposition process from a ceramic target an extensive optimization of the substrate temperature and its influence on the device performance was carried out. It was found that the maximum device efficiency can be achieved at deposition temperatures in the range of 200–250°C. At lower deposition temperatures the conversion efficiency is limited and can be improved after post-annealing the device in air. Sputtering the In_xS_y buffer at higher temperatures than 250°C leads to a deterioration of the $CIGS/In_xS_y$/i-ZnO/ZnO:Al device. The In_xS_y buffer sputtered from ceramic targets tends to yield better results than the reactively sputtered In_xS_y buffer.

The stability of devices with indium sulfide buffer from ceramic target was examined by accelerated lifetime tests and was found to be satisfactory. Transient effects were not observed. The so-called damp-heat test according to IEC 61646 on $10 \times 10\,cm^2$ modules was passed without exceeding the defined power loss of 5%.

6.3. $Zn_{1-x}Mg_xO$ by sputtering

This approach to Cd-free cells is unique as it aims to eliminate rather than replace the buffer layer and its preparation. It requires that the functions of the conventional buffer layer and the functions of the undoped ZnO (i-ZnO) layer be fulfilled by a single layer. The band alignment between the chalcopyrite absorber and ZnO is not favorable and has to be adjusted in the absence of the buffer layer. This is achieved by using $Zn_{1-x}Mg_xO$ with a typical $Mg/(Zn + Mg)$ ratio of 15–30% [74,75].

$Zn_{1-x}Mg_xO$ with an adjustable Mg/Zn ratio can be r.f.-sputtered using a dual target configuration [76]. It was shown that single-phase films with fixed ratio can also be prepared in a reproducible manner by sputtering from a single mixed target [77]. This means that existing production lines could easily be converted to this novel approach simply by substituting a $Zn_{1-x}Mg_xO$ target for the ZnO target and abandoning the buffer layer deposition. In many cases this would result not only in a Cd-free module but also in completely dry in-line manufacturing of the module. Dry processing does not provide the surface cleaning inherent to CBD [18]. Hence, it is important that the absorber surface is not contaminated. In particular, oxidation of the surface by prolonged storage under ambient conditions or by adding oxygen to the sputter gas has to be avoided. During deposition the temperature of the absorber should be kept low to avoid the migration of copper to the surface [78].

A large part of this research has been carried out using $Cu(In,Ga)(S,Se)_2$ absorbers from industrial pilot lines prepared in sequential processing. While the deposition of $Zn_{1-x}Mg_xO$ by sputtering as such has been shown to be a very stable process, the absorber surface properties are very crucial and this can affect reproducibility and yield. The best device results are achieved with a sulfur-rich surface of the absorber. In this case the efficiency can reach around 13%, typically 1–2 points lower than the efficiency of CdS-buffered references [79]. An efficiency of up to 16·1% has been reported for using lab-scale evaporated $Cu(In,Ga)Se_2$ absorbers and doping the absorber surface with zinc [80]. More recently the technology has also been applied to $CuInS_2$ pilot-line absorbers reaching an efficiency of 8·2%, again slightly inferior to the standard device [81]. Generally, the current density can be quite high due to the wide band gap of $Zn_{1-x}Mg_xO$ in comparison to CdS (increased blue response). The open-circuit voltage tends to be somewhat reduced but typically the most significant loss is in the FF.

6.4. Up-scaling and outlook

Magnetron sputtering is a well-developed large-area deposition technology and can be easily implemented in a production line. However, in the case of indium sulfide, even though the deposition process is reproducible when the substrate temperature is well controlled some problems occur. Some of those are, the relatively high purchase cost of the In_2S_3 target and the limited target stability at high power densities, i.e., high deposition rates, which can lead to sulfur loss or even to target fractures. Moreover, the realized CIGS-based devices show limited conversion efficiencies compared to reference cells with the conventional CBD-CdS buffer. Therefore, so far to our knowledge, no attempts for a commercialization of the magnetron sputtered In_xS_y layer as buffer were done.

In the case of $Zn_{1-x}Mg_xO$, no particular problems have been encountered in scaling the technology to monolithically integrated modules of up to $30 \times 30\,cm^2$. The losses in efficiency observed already for lab-scale cells translate to the modules. The results concerning damp-heat stability are not yet fully conclusive but it is believed that sufficiently stable modules can be achieved. In consequence, the final assessment of industrial feasibility depends on whether it will be possible to close the gap in efficiency between the standard device and this novel approach.

In the case of evaporated buffers, no large-area deposition has been yet reported.

7. ATOMIC LAYER DEPOSITION

ALD is a chemical vapor deposition technique, previously known as atomic layer epitaxy (ALE) and atomic layer chemical vapor deposition (ALCVD) [82,83]. In ALD film

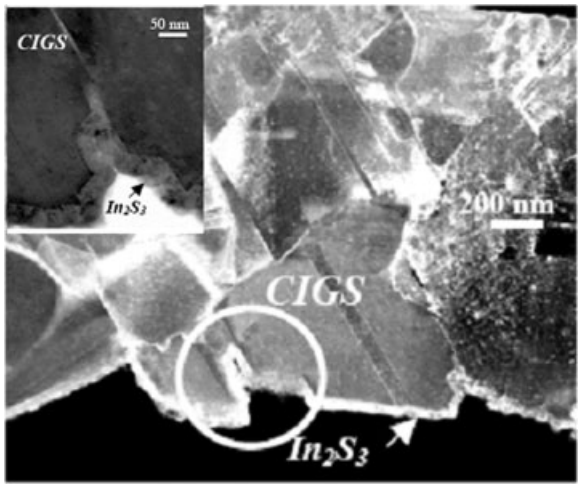

Figure 5. Cross-section TEM micrograph of CIGS + ALD-In_2S_3 thin films [84].

growth takes place from precursors in the vapor phase that are transported into the film deposition zone by an inert carrier gas. The reactants are fed into the reactor separately and sequentially making ALD a pulsed process where chemical reactions on or in the vicinity of the substrate surface control the film growth. Ideally the chemical reactions during each precursor pulse are self-terminating, making the thickness control in ALD very good (Figure 5) [84]. Other advantages are that the method produces films with excellent step coverage and uniformity. The main drawback is that the film growth rate is low compared to other deposition techniques.

High efficiency devices employing buffer layers by ALD are achieved with several materials: Zn(O,S) [85,86], (Zn,Mg)O [87], and In_2S_3[88,89] using co-evaporated CIGS absorbers. There are several reports on relatively efficient devices using ALD-ZnO directly deposited onto the CIGS surface [90,91].

7.1. In_2S_3 buffer layer

The first promising results on ALD-In_2S_3 as buffer layer reached a cell efficiency of 13·5% [92]. A few years later a record efficiency of 16·4% for a laboratory cell was achieved [88].

In all growth studies by different groups, the In_2S_3 films were deposited using indium acetylacetonate and hydrogen sulfide as precursors. The resulting film crystallizes in the β-In_2S_3 structure [93–95]. Deposition temperatures in the range of 120 up to 260°C have been evaluated, where a maximum growth rate between 0·5 and 0·7 Å/cycle at 160–180°C was measured [93–96]. An optimum deposition temperature in the range of 200–220°C was reported with an optimum layer thickness of around 30–50 nm [89,95,97].

Different band-gap values have been reported such as a direct band gap of 2·7–2·8 eV[93,94] and an indirect band gap of 2·1 eV [95]. A higher open-circuit voltage is in most cases observed for high efficient solar cells with the ALD-In_2S_3 buffer than for references with CdS. Quantum efficiency measurements show an improved photocurrent for wavelengths in the range of 300–500 nm, but a loss in higher wavelength regimes compared to the CdS references [88].

7.2. Zn(O,S) buffer layer

Deposition of Zn(O,S) by ALD is reported in Reference [84] and as buffer layer on CIGS for the first time in Reference [92]. The most common precursors are diethyl zinc, H_2S, and H_2O where the film composition can be varied from ZnO to ZnS depending on the pulsing ratio. The band gap varies from 3·3 eV for ZnO to a minimum of about 2·6 eV for $S/(O+S) = 0{\cdot}5$, to 3·6 eV for ZnS. From density functional calculations of the conduction band offset as a function of sulfur content and *in situ* photoemission measurements of the CIGS/Zn(O,S) interface [98,99], a sulfur content of about $0{\cdot}7S/(O+S)$ is expected to result in favorable band alignment needed for efficient devices. A gradient with higher sulfur content close to the absorber was shown, most likely due to a longer incubation time for growth of ZnO on CIGS as compared to ZnS [100,101]. Reproducible results were obtained [102] for 20–50 nm thick Zn(O,S) films with an average S/Zn ratio of 0·2–0·3 but with a more sulfur-rich interface. Cell efficiency of up to 18·5% with AR coating was shown [85] for deposition at 120°C and thickness of about 20 nm. High efficiency was also reported for non-covering and sulfur-rich ALD-Zn(O,S) with an ALD-ZnO top layer [103].

Devices with ALD-Zn(O,S) normally show highest efficiency as-deposited. However, after a few months of storage, degradation in FF has been observed. High FF can be restored by light soaking at an elevated temperature of about 100°C [103], similar to the behavior of as-deposited CBD-Zn(O,S) [104]. Encapsulated modules with ALD-Zn(O,S) buffers have shown superior stability as compared to CBD-Zn(O,S) buffers [86].

7.3. $Zn_{1-x}Mg_xO$ buffer layer

$Zn_{1-x}Mg_xO$ is considered as a buffer layer for CIGS solar cells due to the ability to increase the optical band gap of ZnO by the addition of magnesium. Ohtomo *et al*. [105] showed that the band gap of $Zn_{1-x}Mg_xO$ films grown by pulsed laser deposition (PLD) increases linearly with the magnesium content until phase segregation of cubic MgO occurs. An x-value of 0·33 for single-phase wurtzite films was obtained, corresponding to a band gap of 4·0 eV. By increasing mainly the conduction band of ZnO with inclusion of Mg, improved band alignment with CIGS and thus better device efficiency is expected [106].

An ALD process for $Zn_{1-x}Mg_xO$ buffer layers in the temperature region from 105 up to 180°C has been developed using water, diethyl zinc, and bis-cyclopenta-

DOI: 10.1002/pip.955

dienyl magnesium as source materials [107]. The magnesium content in the $Zn_{1-x}Mg_xO$ films varies both with respect to the Mg/Zn pulse ratio and as a function of deposition temperature. A best cell efficiency of 18·1% with anti-reflective coating for CIGS/ALD-$Zn_{1-x}Mg_xO$ solar cells is reached at a deposition temperature of 120°C on co-evaporated CIGS [87]. The solar-cell device parameters are insensitive to changes in the $Zn_{1-x}Mg_xO$ buffer layer thickness in between 80 and 600 nm. It is also shown that higher efficiency can be obtained by omitting the intrinsic ZnO window layer from the solar-cell structure [87,88]. For $Zn_{1-x}Mg_xO$, a major loss in device efficiency due to lower V_{oc} and FF at deposition temperatures above 150°C is observed for ALD-$Zn_{1-x}Mg_xO$ [108] as well as for sputter deposited $Zn_{1-x}Mg_xO$ on $Cu(In,Ga)(S,Se)_2$ [109]. Efficient $CuGaSe_2$-based cells (6·2%) with direct ALD $Zn_{1-x}Mg_xO$ deposition on the absorber have also been obtained [110].

7.4. Up-scaling and outlook

For Zn(O,S) and In_2S_3, modules of up to $30 \times 30\,cm^2$ in size show efficiencies close to CdS reference values, as well as promising encapsulated stability results [86,89]. Large-area deposition of ZnS using ALD was developed commercially by the Finnish company, Planar, for thin-film electroluminescent displays in the beginning of the 1980s. In 1987, another Finnish company, Microchemistry, was founded with one of the aims being the introduction of ALD in thin-film solar cells [111]. Several ALD companies now exist, focusing on equipment manufacturing or process development for the semiconductor, solar cell, or coating industry. So far, the largest reported CIGS modules using ALD are $30 \times 30\,cm^2$ where the ALD reactor was made by Microchemistry [112].

The drawback of ALD for solar-cell production is mainly the slow deposition rate, which is on the order of a few nanometers per minute. However, for thin buffer layers, the total process time could be acceptable. Other drawbacks can be the relatively high cost of metal organic precursors and the lack of large-area equipment on the market. The advantages such as conformal coverage, low energy deposition, and excellent compositional control for optimal band alignment, are reflected in the high solar-cell efficiencies. Another advantage is the possibility to integrate the buffer deposition in an in-line vacuum system.

8. WINDOW LAYERS

In Cu-chalcopyrite solar cells, the standard cell is a heterojunction following the absorber/window approach where the window has a much wider band gap than the absorber. This moves the absorption maximum into the cell and away from the surface, thereby minimizing the influence of surface recombination. The window must thus be highly transparent, create an interface to the absorber with low recombination losses, and limit the influence of locally distributed shunts and performance fluctuations. In addition, it must have a low sheet resistance to laterally transport the current over macroscopic distances to the nearest metal contact finger or interconnect. However, depositing a film with low lateral resistance directly onto the buffer increases the negative influence of local defects such as pin holes and local fluctuation of absorber properties (e.g., band gap) [113,114]. This can be avoided by first depositing of a thin (100 nm) ZnO film with lower conductivity, designated as i-ZnO. In the classical chalcopyrite cell, the buffer establishes the interface properties, the undoped ZnO (i-ZnO) decouples poorly performing locations, and the highly doped ZnO is responsible for lateral current transport. The requirements for the window layer can be divided into physical properties and technological requirements. Key issues for the industrial success are high deposition rates, homogeneous large-area coating, and high process stability with easy control leading to high yield. Yet the deposition materials and equipment cost should be low and guarantee a high uptime. Because the window layer is deposited after the pn-junction formation the substrate temperatures during deposition are limited to about 200°C in order to avoid detrimental diffusion.

8.1. Undoped oxide buffer layer

It is common to use an undoped high resistivity sputtered ZnO (i-ZnO) before the deposition of the widow layer. This additional buffer layer is usually employed in order to make the pn-junction less sensitive to shunts, material fluctuations of the absorber [7,114], or to protect it against sputter damage by energetic ions. The desired high resistivity of the film is obtained using an undoped ZnO target, if necessary by oxygen admixture to the Ar sputter gas. Because the pure target is not conducting, r.f. sputtering is usually applied. However, for production this is not an appropriate process because of high equipment cost, low deposition rates, and its tendency to strong plasma inhomogeneities. The application of advanced processes such as pulsed d.c. or reactive sputtering are under consideration.

Film thickness of i-ZnO turned out to be of minor influence on cell efficiency when a CdS buffer layer is used and may vary from few to several hundred nanometers. However, optimization concerning both resistivity and thickness is mandatory for monolithical module integration when i-ZnO is deposited *in situ* onto Mo afore the subsequent TCO, thereby inhibiting the Mo-TCO interconnect. In the case of Cd-free buffer layers the undoped buffer layer can strongly influence the performance of cells. As was mentioned previously, for example, for CBD-ZnS buffer layers the replacement of i-ZnO by $Zn_{1-x}Mg_xO$ can improve the efficiency and stability of the cells [32–36]. Moreover, in some applications of CBD-ZnS the best modules are prepared without using this

undoped oxide buffer layer and by depositing the transparent conducting window directly on the buffer layer either by sputtering[27] or by softer methods such as MOCVD [48].

8.2. Transparent conductive window layer (TCO)

The window layer of the chalcopyrite-based solar cells is usually a degenerately doped semiconductor serving both as n^+-type partner in the pn-heterojunction and as a transparent contact layer (TCO). It is obvious that low resistivity together with high transparency from the UV–Visible region up to the absorber band gap in the near IR is necessary. But optimum performance requires good matching of the electronic bands and the lattice constants to the underlying absorber/buffer layers as well.

The most common TCO materials are SnO_2:F (FTO), In_2O_3:Sn (ITO), and highly doped ZnO, namely with gallium (ZGO), aluminum (ZAO), or boron (ZBO) [115]. However, as the deposition of FTO requires deposition temperatures higher than 200°C is not used in chalcopyrite-based devices. ITO and doped ZnO can both be used, but actually the most common material used is ZnO because of its lower material cost [116]. The most commonly used low temperature deposition method for these films is sputtering. However, various other deposition methods have been tested, including MOCVD [117,118], PLD [116], sol–gel method [119], and electrodeposition [120,121]. Though the obtained material quality may be high, some of these techniques are not yet of industrial relevance, because of high process temperatures needed or poor homogeneity on large areas.

For economic and ecological reasons magnetron sputtering of ZnO doped with Al or Ga is the industrial standard today, allowing for high efficiencies at moderate cost. Chalcopyrite-based cells on small areas with the highest efficiencies obtained so far are normally coated by ZnO:Al (ZAO) using r.f. sputtering of high purity $ZnO:Al_2O_3$ targets [1]. According to the needs of an industrial production r.f. sputtering was replaced successfully by d.c. sputtering on larger areas for (sub-)module production using low resistive hot isostatic pressed (HIP) targets [122,123]. The breakthrough for the production was achieved by advances in (pulsed) d.c. power supplies and target manufacturing when much cheaper sintered ZAO targets become available. Provided good cooling of the targets, high power densities far above 10 W/cm^2 lead to dynamic deposition rates exceeding 100 nm m/min. Today's development is directed toward the implementation of (dual) cylindrical magnetrons with target tubes which increase the target utility fraction above 80% and extends the maintenance intervals dramatically.

Further cost reduction is anticipated for the reactive sputtering in d.c. or r.f. mode from metal targets[124] in oxygen-containing atmosphere which is mainly based on the much lower cost of metal target manufacturing by casting or spraying. However, the stability and control of the reactive sputtering process at the optimum working point is much more difficult to achieve as compared to the ceramic target sputtering which is almost self-adjusting. The limited allowable substrate temperature is a major drawback in obtaining homogeneous, high quality films.

For CBD-ZnS buffer layers, in some cases the window layer is directly deposited on the buffer by MOCVD using diethyl zinc and deionized water as precursors with boron doping. This deposition process requires only low substrate temperatures and is successfully applied for thin-film Si solar modules [117,118].

It is important to note that film growth and long-term stability of the TCO depend very much on the CIGS/buffer substrate. The zinc oxide growth tends to maintain and even amplify grain boundaries initiated by the underlying substrate. These grain boundaries are believed to be the major source for the drastic increase of lateral sheet resistance especially under influence of humidity and heat as applied in accelerated lifetime tests according to IEC 61646. Deposition conditions and methods leading to more dense film growth have been recognized to improve ZnO film stability.

9. INTERFACE EFFECTS

9.1. Absorber/buffer interface

The nature of the absorber/buffer heterointerface is crucial for the solar-cell operation. In order to reach high efficiencies, such material interfaces should not favor carrier recombination. The shift of the electrical pn-junction into the absorber layer (i.e., surface inversion) is one possibility to minimize interface recombination. However, this condition is not sufficient. The band alignment at the heterojunction also affects the cells parameters. On one hand, a small conduction band spike, i.e., $0 < \chi_{\text{absorber}} - \chi_{\text{buffer}} < 0{\cdot}2$ (χ being the electron affinity) is beneficial since it tends to enhance the inversion [106]. A higher spike impedes the J_{sc} and FF [106]. On the other hand, a cliff (i.e., $\chi_{\text{absorber}} - \chi_{\text{buffer}} < 0$) reduces the recombination barrier, which lowers the cells performance [125]. The formation of efficient absorber/buffer junctions therefore requires interface engineering, which is realized by varying growth parameters of absorber and buffer with subsequent analysis of the structural, compositional as well as the electronic properties of the heterojunction [96,125–129].

Spectrometric techniques such as inverse photoemission (IPES), ultraviolet (UPS), or X-ray photoelectron spectrometry (XPS) offer the advantage of providing information on both the chemistry and the band structures at the absorber/buffer interface. Transmission electron microscopy (TEM) and its related techniques supply (micro)-structural and compositional properties as well as micrographs of the interface. Also secondary ion mass (SIMS) and sputtered neutral mass spectrometry (SNMS)

have been applied in order to study the composition across the heterojunction.

By combining XPS/UPS measurements and the optical properties of the buffer layer, Platzer-Björkman *et al*. [99] determined the Cu(In,Ga)Se_2/ALD-Zn(S,O) interface composition and band structure. These authors found a gradual increase of the [S]/[O] ratio toward the absorber/buffer interface. Such higher sulfur content close to the absorber offers an enhanced interfacial, spike-like conduction band offset (0·2 eV, see Figure 6). Zn(O,S) buffer layers which are sulfur-rich close to the interface with the absorber, probably present as a ZnS/Zn(O,S) stack, were reported also for CBD-Zn(S,O) by Bär *et al.* [127] and by Sáez-Araoz *et al*. [30] grown on $CuInS_2$ and Cu(In,Ga)$(S,Se)_2$. Moreover, Bär *et al.* [127] found an interdiffusion of Zn and Cu, probably leading to the formation of a $CuInS_2$/$CuInS_2$:Zn/(Zn,Cu)S/ZnS/Zn(S,O) stack. [128] This intermixing is strongly enhanced by post-annealing.[129,130] Nakada *et al*. [28] also concluded that Zn diffuses into the absorber in the case of Cu(In,Ga)Se_2/CBD-Zn(S,O), but in contrast to the reports mentioned above, these authors measured an oxygen enrichment on the buffer side of the interface. These results give rise to the conclusion that the interface composition and hence the band alignment is dependent on both the buffer deposition process and the nature of the absorber.

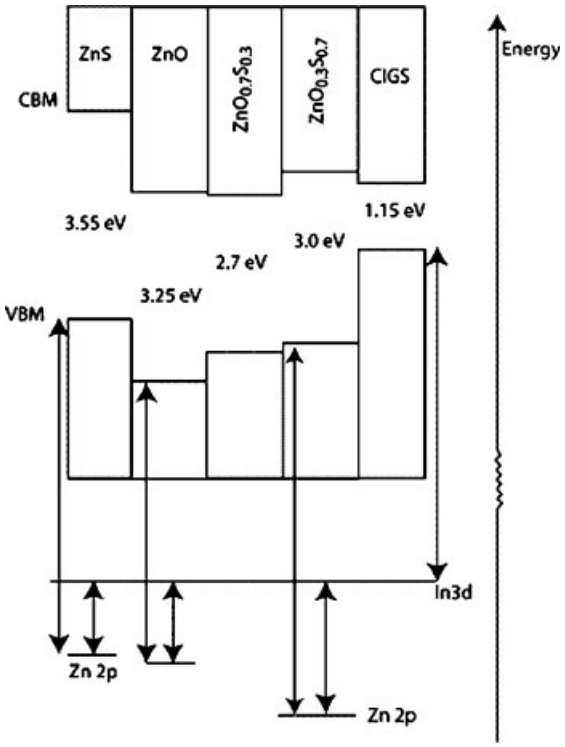

Figure 6. Schematic band diagram (CBM and VBM denote the conduction band minimum and the valence band maximum) of the CIGS/Zn(O,S) interface compared with those of CIGS/ZnO and CIGS/ZnS [99].

For various interfaces formed between Cu(In,Ga)$(S,Se)_2$ and In_2S_3 buffer layers deposited by ALD, co-evaporation (from In and S powders) and compound-evaporation (from In_2S_3 powder), as well as by sputtering and the spray ILGAR technique, it has been reported [68,88,112,129–135] that Cu, and to smaller extent also Ga and Na, diffuses from the absorber into In_2S_3, whereas In diffuses from the buffer into the absorber region close to the interface. Hence, the corresponding solar-cell devices exhibit a Cu-depleted/In-rich region on the absorber side of the absorber/buffer interface and a Cu- (as well as Na- and Ga-) containing In_2S_3 buffer. As Cu and Na occupy the same sites of the In_2S_3 crystal structure [136,137], the amount of Cu diffusing into the buffer also depends on the amount of Na available on the Cu(In,Ga)$(S,Se)_2$ surface prior to the buffer deposition [132,138].

For all the deposition techniques mentioned above, the solar-cell performances deteriorate substantially for In_2S_3 deposition temperatures about 220–250°C. Abou-Ras *et al*. [132,134] related this deterioration to the formation of $CuIn_5S_8$, found in samples with In_2S_3 layers grown above this temperature threshold. $CuIn_5S_8$ is present as an intermediate layer between absorber and In_2S_3 at about 240°C (Reference [132], Figure 7) and replaces In_2S_3 completely for even higher substrate temperatures [133,135]. However, it is not yet understood what impact the $CuIn_5S_8$ formation has on the band alignment between absorber and buffer.

In order to investigate the recombination mechanisms at the Cu(In,Ga)$(S,Se)_2$/In_2S_3 interface, Jacob *et al.* [139] studied the performance of cells with Cu(In,Ga)Se_2/co-evaporated In_2S_3 heterojunctions and varying Ga contents (i.e., varying electron affinity) in the absorbers. These authors concluded that interface recombination dominates for [Ga]/([In] + [Ga]) ratios as low as 0·1. On the other hand, Strohm *et al*. [140] reported that interface recombination is not dominant even for higher Ga contents in the case of cells with Cu(In,Ga)Se_2/compound-evaporated In_2S_3 heterojunctions. Such contradictory results may mean that the recombination mechanism at the Cu(In,Ga)$(S,Se)_2$/In_2S_3 interface depends on the deposition technique of the buffer layer, which determines the properties of the In_2S_3 layers [141] and therefore the properties of the interface formed with the Cu(In,Ga)$(S,Se)_2$.

It may be concluded that in general, the interface formation between the absorber and ZnS or In_2S_3 buffer layers (and therefore the solar-cell performance) depends strongly on the buffer layer deposition technique, the substrate temperature, the supply of Na, and generally the nature of the absorber surface prior to the buffer layer deposition. The small, positive conduction band offset (spike) between Cu(In,Ga)$(S,Se)_2$ and ZnS, probably caused by a S-rich intermediate layer between absorber and buffer, may indicate why solar cells with such heterojunctions reach conversion efficiencies comparable to those with CBD-CdS buffers. In contrast, the heterojunction formed between Cu(In,Ga)$(S,Se)_2$ and In_2S_3

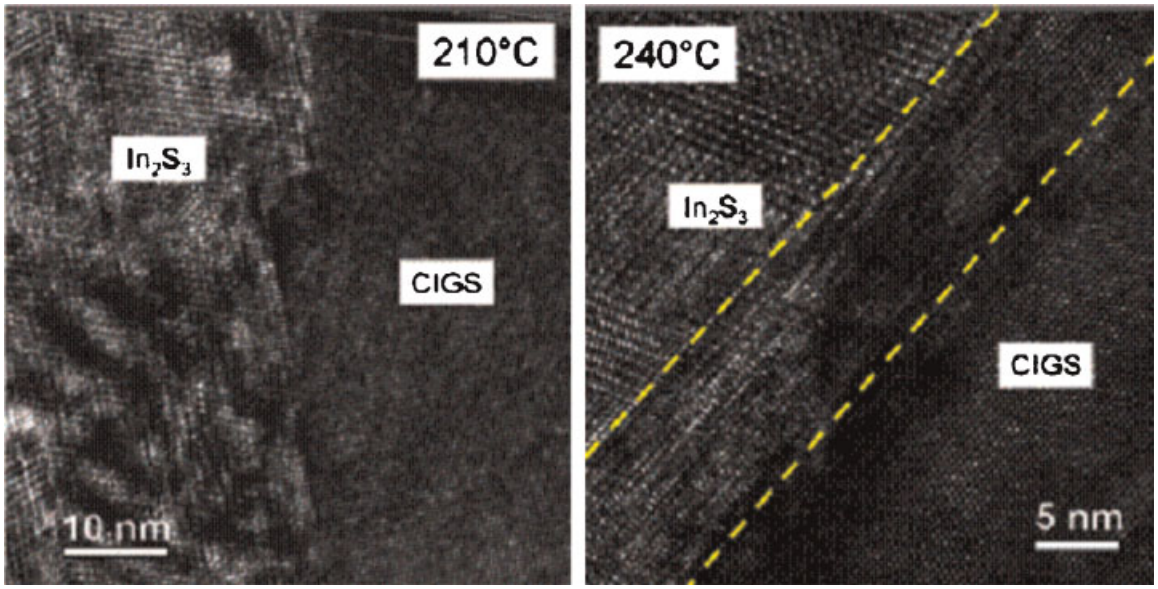

Figure 7. High resolution transmission electron micrograph from the interface of CIGS with In_2S_3 layers grown at 210 and 240°C [131].

needs to be further optimized, which may be complicated by the larger extent of interdiffusion occurring at this interface.

9.2. Buffer/window interface

The surface coverage of a chemically deposited buffer layer is not always perfect, particularly on the grain boundaries or the rough surface of the CIGS layers. This may result in a drop of V_{oc} and FF due to the leakage current between the conductive ZnO:Al and CIGS absorber layers [142]. The local fluctuations in the composition also deteriorate the overall cell performance [114]. In order to overcome these problems, a highly resistive non-doped ZnO thin layer is commonly added between ZnO:Al and the buffer layer for standard CdS/CIGS solar cells. However, the cell performance of some Cd-free devices and especially the CBD-Zn(S,O,OH)-based devices seem to be degraded by plasma damage during ZnO sputtering with the same deposition conditions as those for CdS/CIGS devices [143]. If the ZnO:Al layer is sputter deposited on the Zn(S,O,OH)/CIGSSe, the FF becomes smaller than that of the Zn(S,O,OH)/CIGSSe devices with a ZnO:B window layer deposited by MOCVD, which has no plasma damage.

Although, non-doped ZnO thin layers are not commonly used for Zn(S,O,OH)/CIGS devices, the cell performance should be improved if the ZnO sputtering is done carefully under plasma-reduced conditions. Actually, high efficiency Zn(S,O,OH)/CIGS solar cells were achieved when the non-doped ZnO layer was sputter deposited in a pure Ar gas. In contrast, if the ZnO layer was sputter deposited in a mixture of O_2 and Ar gas, the cell performance was significantly degraded. The *J–V–T* (temperature) analysis suggests that the high efficiency Zn(S,O,OH)/CIGS device is dominated by bulk recombination, whereas the low efficiency cell is dominated by interface recombination due to a large number of defects formed by energetic oxygen ions during sputtering [7]. This result is coherent with a recent finding that the conduction band offset of Zn(S,O,OH)/CIGS is almost the same as that of CdS/CIGS devices as mentioned above [144].

Similar results have been observed for CBD-Zn(S,O,OH) where the sputtered i-ZnO is replaced by sputtered $Zn_{1-x}Mg_xO$ layers [145]. Devices with $Zn_{1-x}Mg_xO$ buffer layers often exhibit pronounced improvements under light soaking, mainly in the FF. For sputtered $Zn_{1-x}Mg_xO$ with intermediate CBD-Zn(S,O,OH) buffer layers [33,146], the same results are observed, while for CBD-Zn(S,O,OH)/i-ZnO both V_{oc} and FF improve after light soaking. For cells with CBD-Zn(S,O,OH)/$Zn_{1-x}Mg_xO$ it was found that recombination losses at the interface are the initially dominant mechanism, which is improved by post-deposition treatments leading to devices controlled by bulk recombination [145]. When only $Zn_{1-x}Mg_xO$ is used as buffer layer the large improvement under light soaking has been suggested to be due to persistent photoconductivity in $Zn_{1-x}Mg_xO$ [147].

10. CONCLUSION AND PERSPECTIVES

The most promising alternative buffer layers developed in the last decade and reaching enough maturity for industrial application are essentially based on In_2S_3, ZnS, ZnMgO, and their oxy-hydroxide derivate compositions. Most of these buffer layers seem, with some deposition techniques, to reach the same/or even better efficiencies than their CdS

Prog. Photovolt: Res. Appl. 2010; **18**:411–433 © 2010 John Wiley & Sons, Ltd.
DOI: 10.1002/pip.955

references. Higher efficiencies than CBD CdS are generally obtained from soft techniques giving conformal depositions such as CBD, ILGAR, or ALD. However, as of today only the CBD-ZnS, CBD-In_2S_3, and ILGAR-In_2S_3 have been implemented in an industrial base-line. For most Cd-free buffer layers even if some technological problems seem to be on the verge of being resolved, such as short deposition time or development of suitable large-area deposition systems, other important technological problems are not yet completely solved such as the need of post-treatment like light soaking or annealing, and long-term stability.

Moreover, even if for CBD-CdS buffers high and reproducible efficiencies are obtained whatever the absorber used, the Cd-free buffer layers seem to be either highly absorber dependent (especially the one based on In_2S_3) or/and there is a need to use a suitable window layer regarding the buffer layer. In summary, while important effort has been made to improve Cd-free efficiencies of cells and modules, some important progress is still needed regarding a better understanding of different interface formations in these cells in order to improve their stabilization for future industrial applications.

REFERENCES

1. Repins I, Contreras MA, Egaas B, DeHart C, Scharf J, Perkins CL, To B, Noufi R. 19.9%-Efficient ZnO/CdS/$CuInGaSe_2$ solar cell with 81.2% fill factor. *Progress in Photovoltaics: Research and Applications* 2008; **16**: 235–239.
2. Kessler J, Wennerberg J, Bodegard M, Stolt L. Highly efficient Cu(In,Ga)Se-2 mini-modules. *Solar Energy Materials & Solar Cells* 2003; **75**: 35–46.
3. Dimmler B, Powalla M, Schaeffler R. CIS solar modules: pilot production at Wuerth Solar. *Conference Record of the Thirty-First IEEE Photovoltaic Specialists Conference*, 2005; 189–194.
4. Hariskos D, Spiering S, Powalla M. Buffer layers in Cu(In,Ga)Se_2 solar cells and modules. *Thin Solid Films* 2005; **480–481**: 99–109.
5. Siebentritt S. Alternative buffers for chalcopyrite solar cells. *Solar Energy* 2004; **77**: 767–775.
6. Rau U, Grabitz PO, Werner JH. Resistive limitations to spatially inhomogeneous electronic losses in solar cells. *Applied Physics Letters* 2004; **85**(24): 6010–6012.
7. Klenk R. Characterisation and modelling of chalcopyrite solar cells. *Thin Solid Films* 2001; **387**: 135–140.
8. Furlong MJ, Froment M, Bernard MC, Cortès R, Tiwari AN, Krejci M, Zogg H, Lincot D. Aqueous solution epitaxy of CdS layers on CdS. *Journal of Crystal Growth* 1998; **193**: 114–122.
9. Niemi E, Stolt L. Characterization of $CuInSe_2$ thin films by XPS. *Surface and Interface Analysis* 1990; **15**: 422–426.
10. Wada T, Hayashi S, Hashimoto Y, Nishiwaki S, Sato T, Negami T, Nishitani M. High efficiency Cu(In, Ga)Se_2 (CIGS) solar cells with improved CIGS surface. *Proceedings of the 2nd World Conference on Photovoltaic Solar Energy Conversion, Vienna*, 1998; 403–408.
11. Persson C, Zhao YJ, Lany S, Zunger A. n-Type doping of $CuInSe_2$ and $CuGaSe_2$. *Physical Review B* 2005; **72**: 035211.
12. Liao D, Rockett A. Cu depletion at the $CuInSe_2$ surface. *Applied Physics Letters* 2003; **82**: 2829–2831.
13. Siebentritt S, Papathanasiou N, Albert J, Lux-Steiner MC. Stability of surfaces in the chalcopyrite system. *Applied Physics Letters* 2006; **88**(15): 1919.
14. Schmid D, Ruckh M, Grunwald F, Schock HW. Chalcopyrite/defect chalcopyrite heterojunctions on the basis of $CuInSe_2$. *Journal of Applied Physics* 1993; **73**(6): 2902–2909.
15. Pistor P, Klenk R. On the advantage of a buried pn-junction in chalcopyrite solar cells: An urban legend? *Proceedings of the International Workshop on Numerical Modelling of Thin Film Solar Cells, Gent, Belgium, Burgelman M, Topic (Ed.)*, 2007; 179–182.
16. Todorov T, Carda J, Escribano P, Grimm A, Klaer J, Klenk R. Electrodeposited In_2S_3 buffer layers for $CuInS_2$ solar cells. *Solar Energy Materials & Solar Cells* 2008; **92**(10): 1274–1278.
17. Spiering S, Bürkert L, Hariskos D, Powalla M, Dimmler B, Giesen C, Heuken M. MOCVD indium sulphide for application as a buffer layer in CIGS solar cells. *Thin Solid Films* 2009; **517**(7): 2328–2331.
18. Kessler J, Velthaus KO, Ruckh M, Laichinger R, Schock HW, Lincot D, Ortega R, Vedel J. Chemical bath deposition of CdS on $CuInSe_2$, etching effects and growth kinetics. *Proceedings of the International PVSEC-6, New Delhi*, 1992; 1005–1010.
19. Nakada F. Improved efficiency of Cu(In,Ga)Se_2 thin film solar cells with chemically deposited ZnS buffer layers by air-annealing – formation of homojunction by solid phase diffusion. *Proceedings of the 28th IEEE Photovoltaic Specialists Conference*, 2000; 529–534.
20. Nakada T, Kunioka A. Direct evidence of Cd diffusion into CIGS thin films during chemical-bath deposition process of CdS films. *Applied Physics Letters* 1999; **74**(17): 2444–2446.
21. Ortega Borges R, Lincot D, Vedel J. Chemical bath deposition of zinc sulfide thin films. *Proceedings of the 11th EC PVSEC, Montreux, Switzerland*, 1992; 862–865.
22. Kessler J, Ruckh M, Hariskos D, Rühle U, Menner R, Schock HW. Interface engineering between $CuInSe_2$ and ZnO. *Proceedings of the 23rd EC PVSEC, Louisville*, 1993; 447–452.
23. Kushiya K, Nii T, Sugiyama I, Sata Y, Inamori Y, Takeshita H. Application of Zn-compound buffer

layer for polycrystalline $CuInSe_2$-based thin-film solar cells. *Japanese Journal of Applied Physics* 1996; **35**: 4383–4388.
24. Nakada T, Mizutani M, Hagiwara Y, Kunioka A. High-efficiency $Cu(In,Ga)Se_2$ thin-film solar cells with a CBD-ZnS buffer layer. *Solar Energy Materials & Solar Cells* 2001; **67**: 255–260.
25. Nakada T, Mizutani M. 18% Efficiency Cd-free $Cu(In, Ga)Se_2$ thin-film solar cells fabricated using chemical bath deposition (CBD)-ZnS buffer layers. *Japanese Journal of Applied Physics* 2002; **41**: L165–L167.
26. Contreras MA, Nakada T, Hongo M, Pudov AO, Sites JR. $ZnO/ZnS(O,OH)/Cu(In,Ga)Se_2$/Mo solar cells with 18.6% efficiency. *Proceedings of the 3rd World Conference of Photovoltaic Energy Conversion (WCPEC-3)*, Osaka, Japan, 2003; 570–573.
27. Bhattacharya RN, Contreras MA, Teeter G. 18.5% Copper indium gallium diselenide (CIGS) device using single-layer chemical-bath-deposited ZnS(O, OH). *Japanese Journal of Applied Physics* 2004; **43**(11B): L1475–L1476.
28. Nakada T, Hongo M, Hayashi E. Band offset of high efficiency CBD-ZnS/CIGS thinfilm solar cells. *Thin Solid Films* 2003; **431/432**: 242–248.
29. Ennaoui A, Bär M, Klaer J, Kropp T, Sáez-Araoz R, Lux-Steiner MC. Highly-efficient Cd-free $CuInS_2$ thin-film solar cells and mint-modules with Zn(S,O) buffer layers prepared by an alternative chemical bath process. *Progress in Photovoltaics: Research and Applications* 2006; **14**: 499–511.
30. Sáez-Araoz R, Abou-Ras D, Niesen TP, Neisser A, Wilchelmi K, Lux-Steiner MC, Ennaoui A. In situ monitoring the growth of thin-film ZnS/Zn(S,O) bilayer on Cu-chalcopyrite for high performance thin film solar cells. *Thin Solid Films* 2009; **517**(7): 2300–2304.
31. Sáez-Araoz R, Ennaoui A, Kropp T, Veryaeva E, Niesen TP, Lux-Steiner MC. Use of different Zn precursors for the deposition of Zn(S,O) buffer layers by chemical bath for chalcopyrite based Cd-free thin-film solar cells. *Physica Status Solidi A* 2008; **205**(10): 2330–2334.
32. Hariskos D, Fuchs B, Menner R, Powalla M, Naghavi N, Lincot D. The ZnS/ZnMgO buffer combination in CIGS-based solar cells. *Proceedings of the 22nd European Photovoltaic Solar Energy Conference*, 2007; 1907–1910.
33. Hariskos D, Fuchs B, Menner R, Powalla M, Naghavi N, Hubert C, Lincot D. The Zn(S,O,OH)/ZnMgO buffer in thin film $Cu(In,Ga)(S,Se)_2$-based solar cells. Part II: Magnetron sputtering of the ZnMgO buffer layer for in-line co-evaporated $Cu(In,Ga)Se_2$ solar cells. *Progress in Photovoltaics: Research and Applications* 2009; **17**: 479–488.
34. Hubert C, Naghavi N, Etcheberry A, Roussel O, Hariskos D, Powalla M, Kerrec O, Lincot D. A better understanding of the growth mechanism of Zn(S,O,OH) chemical bath deposited buffer layers for high efficiency $Cu(In,Ga)(S,Se)_2$ solar cells. *Physica Status Solidi A* 2008; **205**(10): 2335–2339.
35. Hubert C, Naghavi N, Roussel O, Etcheberry O, Hariskos D, Menner R, Powalla M, Kerrec O, Lincot D. The Zn(S,O,OH)/ZnMgO buffer in thin film $Cu(In,Ga)(S,Se)_2$-based solar cells. Part I: Fast chemical bath deposition of Zn(S,O,OH) buffer layers for industrial application on co-evaporated $Cu(In,Ga)Se_2$ and electrodeposited $CuIn(S,Se)_2$ solar cells. *Progress in Photovoltaics: Research and Applications* 2009; **17**: 470–478.
36. Witte W, Hariskos D, Kniese R, Powalla M. Short-circuit current improvement of $CuGaSe_2$ solar cells with a ZnS/(Zn,Mg)O buffer combination. *Physica Status Solidi RRL* 2008; **2**(2): 80–82.
37. Minemoto T, Takakura H, Hamakawa Y, Hashimoto Y, Nishiwaki S, Negami T. Highly efficient Cd-free $Cu(In,Ga)Se_2$ solar cells using novel window layer of (Zn,Mg)O films. *Proceedings of the 16th European Photovoltaic Solar Energy Conference*, 2000; 686–689.
38. Hariskos D, Ruckh M, Rühle U, Walter T, Schock HW, Hedström J, Stolt L. A novel cadmium free buffer layer for $Cu(In,Ga)Se_2$ based solar cells. *Solar Energy Materials & Solar Cells* 1996; **41–42**: 345–353.
39. Bayón R, Guillén C, Martínez MA, Gutiérrez MT, Herrero J. Preparation of indium hydroxy sulfide $In_x(OH)_yS_z$ thin films by chemical bath deposition. *Journal of the Electrochemical Society* 1998; **145**: 2775–2779.
40. Bayón R, Hernández-Mayoral M, Herrero J. Growth mechanism of CBD-$In(OH)_xS_y$ thin films. *Journal of the Electrochemical Society* 2002; **149**: C59–C67.
41. Asenjo B, Chaparro AM, Gutiérrez MT, Herrero J. Quartz crystal microbalance study of the growth of indium(III) sulphide films from a chemical solution. *Electrochimica Acta* 2004; **49**: 737–744.
42. Asenjo B, Sanz C, Guillén C, Chaparro AM, Herrero J, Gutiérrez MT. Indium sulfide buffer layers deposited by dry and wet methods. *Thin Solid Films* 2007; **515**: 6041–6044.
43. Bayón R, Herrero J. Structure and morphology of the indium hydroxy sulphide thin films. *Applied Surface Science* 2000; **158**: 49–57.
44. Asenjo B, Chaparro AM, Gutiérrez MT, Herrero J, Klaer J. Influence of In_2S_3 film properties on the behavior of $CuInS_2/In_2S_3$/ZnO type solar cells. *Solar Energy Materials & Solar Cells* 2005; **87**: 647–656.
45. Asenjo B, Chaparro AM, Gutiérrez MT, Herrero J, Klaer J. Growth and properties of In_2S_3 thin films for buffer layers of $CuInS_2$ based solar cells. *Proceedings of the 19th European Photovoltaic Solar Energy Conference*, 2004; 1784–1787.
46. Asenjo B, Chaparro AM, Gutiérrez MT, Herrero J, Klaer J. Study of $CuInS_2$/buffer/ZnO solar cells, with

chemically deposited ZnS-In_2S_3 buffer layers. *Thin Solid Films* 2007; **515**: 6036–6040.
47. Bayón R, Guillén C, Martínez MA, Chaparro AM, Gutiérrez MT, Herrero J. Different substrates for indium hydroxy sulphide thin films CBD-prepared. Approach to large-area deposition. *Proceedings of the 2nd World Conference on Photovoltaic Solar Energy Conversion*, 1998; 636–639.
48. Kushiya K, Tanaka Y, Hakuma H, Goushi Y, Kijima S, Aramoto T, Fujiwara Y. Interface control to enhance the fill factor over 0.70 in a large-area CIS-based thin-film PV technology. *Thin Solid Films* 2009; **517**(7): 2108–2110.
49. Fischer C-H, Muffler H-J, Lux-Steiner MC. Verfahren zur Herstellung dünner, schwer löslicher Beschichtungen, amtl. Aktenzeichen: DE 50000 568T2 (2002) and International Patents; Fischer C-H, Lux-Steiner MC, Möller J, Könenkamp R, Siebentritt, S,Verfahren und Anordnung zur Herstellung dünner Metallchalkogenid-Schichten DE 59914444.0-08T2 (2007) and International Patents.
50. Bär M, Fischer C-H, Muffler H-J, Zweigart S, Karg F, Lux-Steiner MC. Replacement of the CBD-CdS buffer and the sputtered i-ZnO by an ILGAR-ZnO WEL: optimisation of the WEL deposition. *Solar Energy Materials & Solar Cells* 2003; **75**: 101–107.
51. Bär M, Bloeck U, Muffler HJ, Lux-Steiner MC, Fischer CH, Giersig M, Niesen TP, Karg F. Cd^{2+}/NH_3-treatment of Cu(In,Ga)$(S,Se)_2$: impact on the properties of ZnO layers deposited by the ion layer gas reaction method. *Journal of Applied Physics* 2005; **97**(1): 014905.
52. Allsop NA, Schönmann A, Belaidi A, Muffler H-J, Mertesacker B, Bohne W, Strub E, Röhrich J, Lux-Steiner MC, Fischer C-H. Indium sulfide thin films deposited by the spray ion layer gas reaction technique. *Thin Solid Films* 2006; **3**: 52–56.
53. Allsop NA, Schönmann A, Muffler H-J, Bär M, Lux-Steiner MC, Fischer C-H. Spray-ILGAR indium sulfide buffers for Cu(In,Ga)$(S,Se)_2$ solar cells. *Progress in Photovoltaics: Research and Applications* 2005; **13**: 607–616.
54. Allsop NA, Hänsel A, Visbeck S, Niesen TP, Lux-Steiner MC, Fischer C-H. The dry and damp heat stability of chalcopyrite solar cells prepared with an indium sulfide buffer deposited by the spray-ILGAR technique. *Thin Solid Films* 2006; **511–512**: 55–59.
55. Bär M, Allsop NA, Lauermann I, Fischer C-H. Deposition of In_2S_3 on Cu(In,Ga)$(S,Se)_2$ thin film solar cell absorbers by spray ion layer gas reaction: evidence of strong interfacial diffusion. *Applied Physics Letters* 2007; **90**: 132118.
56. Allsop NA, Camus C, Hänsel A, Gledhill SE, Lauermann I, Lux-Steiner MC, Fischer CH. Indium sulfide buffer/CIGSSe interface engineering: improved cell performance by the addition of zinc sulfide. *Thin Solid Films* 2007; **515**: 6068–6072.
57. Allsop NA, Camus C, Gledhill SE, Unold T, Lux-Steiner MC, Niesen TP, Fischer CH. Nanostructured ZnS:In2S3 buffer layers on Cu(In,Ga)$(S,Se)_2$: Can voltage and efficiency be improved through interface inhomogeneities on a scale below the minority carrier diffusion length? *Materials Research Society Symposium Proceedings* 2007; **1012**: 43–49.
58. Allsop NA, Niesen TP, Lux-Steiner MC, Fischer CH. Scale up of the spray-ILGAR indium sulfide process for Cu(In,Ga)(S,Se)2 mini-modules prepared using the Spray-ILGAR process. *IEEE Photovoltaics Conference Proceedings* 2009; (submitted).
59. Chamberlin RR, Skarman JS. Chemical spray deposition process for inorganic films. *Journal of the Electrochemical Society* 1966; **113**: 36.
60. Blandenet G, Court M, Lagarde Y. Thin layers deposited by the pyrolysis process. *Thin Solid Films* 1981; **77**: 81–90.
61. Kim WT, Kim CD. Optical-energy gaps of β-In_2S_3 thin films grown by spray pyrolysis. *Journal of Applied Physics* 1986; **60**(7): 2631–2633.
62. Ernits K, Bremaud D, Buecheler S, Hibberd CJ, Kaelin M, Khrypunov G, Mueller U, Mellikov E, Tiwari AN. Characterization of ultrasonically sprayed In_xS_y buffer layers for Cu(In,Ga)Se_2 solar cells. *Thin Solid Films* 2007; **515**: 6051–6054.
63. Buecheler S, Corica D, Guettler D, Chirila A, Verma R, Müller U, Niesen TP, Palm J, Tiwari AN. Ultrasonically sprayed indium sulfide buffer layers for Cu(In,Ga)$(S,Se)_2$ thin-film solar cells. *Thin Solid Films* 2009; **517**(7): 2312–2315.
64. Patil PS. Versatility of chemical spray pyrolysis technique. *Materials Chemistry and Physics* 1999; **59**: 185–198.
65. Gall S, Barreau N, Jacob F, Harel S, Kessler J. Influence of sodium compounds at the Cu(In, Ga)Se_2/(PVD)In_2S_3 interface on solar cell properties. *Thin Solid Films* 2007; **515**: 6076–6079.
66. Pistor P, Caballero R, Hariskos D, Izquierdo-Roca V, Wächter R, Schorr S, Klenk R. Quality and stability of compound indium sulfide as source material for buffer layers in Cu(In,Ga)Se_2 solar cells. *Solar Energy Materials & Solar Cells* 2009; **93**: 148–152.
67. Spiering S, Chowdhury S, Dresel A, Hariskos D, Eicke A, Powalla M. *Evaporated indium sulfide as buffer layer in Cu(In,Ga)Se_2-based solar cells. Proceedings of the 21st European Solar Energy Conference, Dresden, Germany*, 2006; 1847–1852.
68. Eicke A, Spiering S, Dresel A, Powalla M. Chemical characterization of evaporated In_2S_x buffer layers in Cu(In,Ga)Se_2 thin-film solar cells with SNMS and SIMS. *Surface and Interface Analysis* 2008; **40**: 830–833.
69. Gall S, Barreau N, Harel S, Bernède JC, Kessler J. Material analysis of PVD-grown indium sulphide buffer layers for Cu(In,Ga)Se_2-based solar cells. *Thin solid films* 2005; **480–481**: 138–141.

70. Strohm A, Eisenmann L, Gebhardt RK, Harding A, Schlötzer T, Abou-Ras D, Schock HW. $ZnO/In_xS_y/Cu(In,Ga)Se_2$ solar cells fabricated by coherent heterojunction formation. *Thin Solid Films* 2005; **480–481**: 162–167.
71. Abous-Ras D, Kostorz G, Strohm A, Schock HW, Tiwari AN. Interfacial layer formations between $Cu(In,Ga)Se_2$ and InxSy layers. *Journal of Applied Physics* 2005; **98**: 123512-1-7.
72. Hariskos D, Menner R, Spiering S, Eicke A, Powalla M, Ellmer K, Oertel M, Dimmler B. In_2S_3 buffer layer deposited by magnetron sputtering for $Cu(In-Ga)Se_2$ sollar cells. *Proceedings of the 19th European Photovoltaic Solar Energy Conference*, 2004; 1894–1897.
73. Hariskos D, Menner R, Lotter E, Spiering S, Powalla M. Magnetron sputtering of indium sulphide as the buffer layer in $Cu(InGa)Se_2$-based solar cells. *Proceedings of the 20th European Photovoltaic Solar Energy Conference*, 2005; 1713–1716.
74. Negami T, Minemoto T, Hashimoto Y, Satoh T. CIGS solar cells using a novel window $Zn_{1-x}Mg_xO$ film. *Proceedings of the 28th IEEE Photovoltaic Specialists Conference*, 2000; 634–637.
75. Glatzel T, Steigert H, Sadewasser S, Klenk R, Lux-Steiner MC. Potential distribution of $Cu(In,-Ga)(S,Se)_2$-solar cell cross-sections measured by Kelvin probe force microscopy. *Thin Solid Films* 2005; **480–481**: 177–182.
76. Minemoto T, Negami T, Nishiwaki S, Takakura H, Hamakawa Y. Preparation of $Zn_{1-x}Mg_xO$ films by radio frequency magnetron sputtering. *Thin Solid Films* 2000; **372**: 173–176.
77. Glatzel T, von Roon S, Sadewasser S, Klenk R, Jäger-Waldau A, Lux-Steiner MC. (Zn,Mg)O as window layer for Cd-free chalcopyrite solar cells. *Proceedings of the 17th European Photovoltaic Solar Energy Conference and Exhibition*, Munich, 2001; 1151–1154.
78. Lauermann I, Loreck C, Grimm A, Klenk R, Mönig H, Lux-Steiner MC, Fischer CH, Visbeck S, Niesen TP. Cu-accumulation at the interface between sputter-(Zn,Mg)O and $Cu(In,Ga)(S,Se)_2$ – A key to understanding the need for buffer layers? *Thin Solid Films* 2007; **515**: 6015–6019.
79. Glatzel T, Steigert H, Klenk R, Lux-Steiner MC, Niesen TP, Visbeck S. $Zn_{1-x}Mg_x$ as a window layer in completely Cd-free $Cu(In,Ga)(S,Se)_2$ based thin film solar cells. *Technical Digest of the International PVSEC-14, Bangkok*, 2004; 707–708.
80. Negami T, Aoyagi T, Satoh T, Shimakawa SI, Hayashi S, Hashimoto Y. Cd-free CIGS solar cells fabricated by dry process. *Proceedings of the 29th IEEE Photovoltaic Specialists Conference*, 2002; 656–659.
81. Grimm A, Klenk R, Klaer J, Lauermann I, Meeder A, Voigt S, Neisser A. An alternative window layer concept for chalcopyrite-based thin film solar cells. *Presented at the 2nd International Symposium on Transparent Conductive Oxides*, Hersonissos, 2008.
82. Puurunen R. Surface chemistry of atomic layer deposition: a case study for the trimethylaluminum/water process. *Journal of Applied Physics* 2005; **97**: 121301.
83. Ritala M, Leskelä M. Handbook of Thin Film Materials. Academic Press: San Diego, 2001.
84. Naghavi N, Spiering S, Powalla M, Canava B, Taisne A, Guillemoles JF, Taunier S, Etcheberry A, Lincot D. Toward better understanding of high efficiency Cd-free solar cells using atomic layer deposition indium sulphide buffer layers. *Materials Research Society Symposium Proceedings* 2003; **763**: B9.9.1.
85. Zimmermann U, Ruth M, Edoff M. Cadmium-free CIGS mini-modules with ALD-grown Zn(O,S)-based buffer layers. *Proceedings of the 21st European Photovoltaic Solar Energy Conference*, 2006; 1831–1834.
86. Powalla M, Dimmler B, Gros KH. CIS thin-film solar modules – an example of remarkable progress in PV. *Proceedings of the 20th European Photovoltaic Solar Energy Conference*, 2005; 1689–1694.
87. Hultqvist A, Platzer-Björkman C, Törndahl T, Ruth M, Edoff M. Optimization of i-ZnO window layers for $Cu(In,Ga)Se_2$ solar cells with ALD buffers. *Proceedings of the 22nd European Photovoltaic Solar Energy Conference*, 2007; 2381–2384.
88. Naghavi N, Spiering S, Powalla M, Canava B, Lincot D. High-efficiency copper indium gallium diselenide (CIGS) solar cells with indium sulfide buffer layer deposited by atomic layer chemical vapor deposition (ALCVD). *Progress in Photovoltaics: Research and Applications* 2003; **11**: 437–443.
89. Spiering S, Hariskos D, Schröder S, Powalla M. Stability behaviour of Cd-free CIGS solar modules with In2S3 buffer layer prepared by atomic layer deposition. *Thin Solid Films* 2005; **480–481**: 195–198.
90. Lujala V, Skarp J, Tammenmaa M, Suntola T. Atomic layer epitaxy growth of doped zinc oxide thin films from organometals. *Applied Surface Science* 1994; **82/83**: 34–40.
91. Chaisitsak S, Sugiyama T, Yamada A, Konagai M. $Cu(In,Ga)Se_2$ thin film solar cells with high resistivity ZnO buffer layers deposited by atomic layer deposition. *Japanese Journal of Applied Physics* 1999; **38**: 4989–4992.
92. Yousfi E, Asikainen T, Pietu V, Cowache P, Powalla M, Lincot D. Cadmium-free buffer layers deposited by atomic layer epitaxy for copper indium diselenide solar cells. *Thin Solid Films* 2000; **361–362**: 183–186.
93. Donsanti F, Weinberger B, Cowache P, Bernard M, Lincot D. Atomic layer deposition of indium sulfide layers for copper indium gallium diselenide solar cells. *Proceedings of the Materials Research Society Symposium*, San Francisco, 2001; H8.20.1-8.
94. Naghavi N, Henriquez R, Laptev V, Lincot D. Growth studies and characterisation of In_2S_3 thin

films deposited by atomic layer deposition (ALD). *Applied Surface Science* 2004; **222**: 65–73.
95. Sterner J, Malmström J, Stolt L. Study on ALD In_2S_3/$Cu(In,Ga)Se_2$ interface formation. *Progress in Photovoltaics: Research and Applications* 2005; **13**: 179–193.
96. Spiering S, Hariskos D, Powalla M, Naghavi N, Lincot D. Cd-free $Cu(In,Ga)Se_2$ thin film solar modules with In_2S_3 buffer layer by ALCVD. *Thin Solid Films* 2003; **431–432**: 359–363.
97. Sanders B, Kitai A. Zinc oxysulfide thin films grown by atomic layer deposition. *Chemistry of Materials* 1992; **4**: 1005–1011.
98. Persson C, Platzer-Björkman C, Malmström J, Törndahl T, Edoff M. Strong valence-band offset bowing of $ZnO_{1-x}S_x$ enhances p-type nitrogen doping of ZnO-like alloys. *Physical Review Letters* 2006; **97**: 146403.
99. Platzer-Björkman C, Törndahl T, Abou-Ras D, Malmström J, Kessler J, Stolt L. Zn(O,S) buffer layers by atomic layer deposition in $Cu(In,Ga)Se_2$ based thin film solar cells: band alignment and sulfur gradient. *Journal of Applied Physics* 2006; **100**: 044506.
100. Yousfi E, Fouache J, Lincot D. Study of atomic layer epitaxy of zinc oxide by in-situ quartz crystal microgravimetry. *Applied Surface Science* 2000; **153**: 223–234.
101. Sterner J, Platzer-Björkman C, Stolt L. XPS/UPS monitoring of ALCVD ZnO growth on $Cu(In,Ga)Se_2$ absorbers. *Proceedings of the 17th European Photovoltaic Solar Energy Conference*, Munich, 2001; 1118–1121.
102. Platzer-Björkman C, Törndahl T, Kessler J, Stolt L. Reproducibility of CIGS based solar cells with ALD Zn(O,S) buffer layers. *Proceedings of the 20th European Photovoltaic Solar Energy Conference*, Barcelona, 2005; 1709–1712.
103. Platzer-Björkman C, Kessler J, Stolt L. Atomic layer deposition of Zn(O,S) buffer layers for high efficiency $Cu(In,Ga)Se_2$ solar cells. *Proceedings of the 3rd World Conference on Photovoltaic Energy Conversion*, Osaka, 2003; 461–464.
104. Kushiya K, Yamase O. Stabilization of PN heterojunction between $Cu(In,Ga)Se_2$ thin-film absorber and ZnO window layer with $Zn(O,S,OH)_x$ buffer. *Japanese Journal of Applied Physics* 2000; **39**: 2577–2582.
105. Ohtomo A, Kawasaki M, Koida T, Masubuchi K, Koinuma H. $Mg_xZn_{1-x}O$ as a II–VI widegap semiconductor alloy. *Applied Physics Letters* 1998; **72**: 2466–2468.
106. Minemoto T, Matsui T, Takakura H, Hamakawa Y, Negami T, Hashimoto Y, Uenoyama T, Kitagawa M. Theoretical analysis of the effect of conduction band offset of window/CIS layers on performance of CIS solar cells using device simulation. *Solar Energy Materials & Solar Cells* 2001; **67**: 83–88.
107. Törndahl T, Platzer-Björkman C, Kessler J, Edoff M. Atomic layer deposition of $Zn_{1-x}Mg_xO$ buffer layers for $Cu(In,Ga)Se_2$ solar cells. *Progress in Photovoltaics: Research and Applications* 2006; **15**: 225–235.
108. Törndahl T, Coronel E, Hultqvist A, Platzer-Björkman C, Leifer K, Edoff M. The effect of $Zn_{1-x}Mg_xO$ buffer layer deposition temperature on $Cu(In,Ga)Se_2$ solar cells: a study of the buffer/absorber interface. *Progress in Photovoltaics: Research and Applications* 2009; **17**: 115–125.
109. Lauermann I, Loreck C, Grimm A, Klenk R, Mönig H, Lux-Steiner MC, Fischer C, Visbeck S, Niesen T. Cu-accumulation at the interface between sputter-(Zn,Mg)O and $Cu(In,Ga)(S,Se)_2$ – A key to understanding the need for buffer layers? *Thin Solid Films* 2007; **515**: 6015–6019.
110. Hultqvist A, Platzer-Björkman C, Pettersson J, Törndahl T, Edoff M. $CuGaSe_2$ solar cells using atomic layer deposited Zn(O,S) and (Zn,Mg)O buffer layers. *Thin Solid Films* 2007; **515**(15): 6024–6027.
111. Skarp J, Soininen PJ, Soininen PT. ALE reactor for large area depositions. *Applied Surface Science* 1997; **112**: 251–254.
112. Spiering S, Eicke A, Hariskos D, Powalla M, Naghavi N, Lincot D. Large-area Cd-free CIGS solar modules with In_2S_3 buffer layer deposited by ALCVD. *Thin Solid Films* 2004; **451–452**: 562–566.
113. Rau U, Schmidt M. Electronic properties of ZnO/CdS/$Cu(In,Ga)Se_2$ solar cells-aspects of heterojunction formation. *Thin Solid Films* 2001; **387**: 141–146.
114. Grabitz PO, Rau U, Werner JH. Electronic inhomogeneities and the role of the intrinsic ZnO layer in $Cu(In,Ga)Se_2$ thin film solar cells. *20th European Photovoltaic Solar Energy Conference*, 2005; 1771–1774.
115. Gordon R. Criteria for choosing transparent conductors. *MRS Bulletin* 2000; **25**: 52–57.
116. Fortunato E, Ginley D, Hosono H, Paine DC. Transparent conducting oxides for photovoltaics. *MRS Bulletin* 2007; **32**(3): 242–247.
117. Zimin D. Properties of large area (1.4 m^2) LP-CVD ZnO layers deposited by TCO 1200 production tool. *Proceedings of the 23th European Photovoltaic Solar Energy Conference*, 2008; 2494–2496.
118. Kushiya K, Tachiyuki M, Nagoya Y, Fujimaki A, Sang B, Okumura D, Dsatoh M, Yamase O. Progress in large-area $Cu(InGa)Se_2$-based thin-film modules with a Zn(O,S,OH)x buffer layer. *Solar Energy Materials & Solar Cells* 2001; **67**(1–4): 11–20.
119. Lin KM, Tsai P. Parametric study on preparation and characterization of ZnO:Al films by sol–gel method for solar cells. *Material Science and Engineering B* 2007; **139**(1): 81–87.
120. Rousset J, Saucedo E, Lincot D. Extrinsic doping of electrodeposited zinc oxide films by chlorine for transparent conductive oxide applications. *Chemistry of Materials* 2009; **21**(3): 534–540.
121. Wellings JS, Samantilleke AP, Warren P, Heavens SN, Dharmadasa IM. Comparison of electrodepos-

ited and sputtered intrinsic and aluminium-doped zinc oxide thin films. *Semiconductor Science and Technology* 2008; **23**(12): 125003.
122. Kluth O, Schoepe G, Rech B, Menner R, Oertel M, Orgassa K, Schock HW. Comparative material study on RF and DC magnetron sputtered ZnO:Al films. *Thin Solid films* 2006; **502**(1–2): 311–316.
123. Herrmann D, Oertel M, Menner R, Powalla M. Analysis of relevant plasma parameters for ZnO:Al film deposition based on data from reactive and non-reactive DC magnetron sputtering. *Surface & Coatings Technology* 2003; **174**: 229–234.
124. May C, Menner R, Struempfel J, Oertel M, Sprecher B. Deposition of TCO films by reactive magnetron sputtering from metallic Zn:Al alloy targets. *Surface & Coatings Technology* 2003; **169**: 512–516.
125. Fischer CH, Bär M, Glatzel T, Lauermann I, Lux-Steiner MC. Interface engineering in chalcopyrite thin film solar devices. *Solar Energy Materials & Solar Cells* 2006; **90**(10): 1471–1485. 10.1016/j.solmat.2005.10.012.
126. Bär M, Ennaoui A, Klaer J, Kropp T, Sáez-Araoz, Allsop N, Lauermann I, Schock HW, Lux-Steiner MC. Formation of a ZnS/Zn(S,O) bilayer buffer on $CuInS_2$ thin film solar cell absorbers by chemical bath deposition. *Journal of Applied Physics* 2006; **99**: 123503-1-9. 10.1063/1.2202694.
127. Bär M, Ennaoui A, Klaer J, Kropp T, Saez-Araoz R, Lehmann S, Grimm A, Lauermann I, Loreck C, Sokoll S, Schock HW, Fischer CH, Lux-Steiner MC, Jung C. Intermixing at the heterointerface between ZnS/Zn(S,O) bilayer buffer and $CuInS_2$ thin film solar cell absorber. *Journal of Applied Physics* 2006; **100**: 064911-1-9. 10.1063/1.2345034.
128. Bär M, Ennaoui A, Klaer J, Sáez-Araoz R, Kropp T, Weinhardt L, Heske C, Lux-Steiner MC. The electronic structure of the [Zn(S,O)/ZnS]/$CuInS_2$ heterointerface – impact of post-annealing. *Chemical Physics Letters* 2006; **433**: 71–74.
129. Bär M, Reichardt J, Grimm A, Kötschau I, Lauermann I, Rahne K, Sokoll S, Lux-Steiner MC, Fischer CH, Weinhardt L, Umbach E, Heske C, Jung C, Niesen TP, Visbeck S. Zn(O,OH) layers in chalcopyrite thin film solar cells: valence band maximum versus composition. *Journal of Applied Physics* 2005; **98**: 053702-1-8. 10.1063/1.2034650.
130. Barreau N, Bernède JC, Marsillac S, Amory C, Shafarman WN. New Cd-free buffer layer deposited by PVD: In_2S_3 containing Na compounds. *Thin Solid Films* 2003; **431–432**: 326–329. 10.1016/S0040-6090(03)00216-5.
131. Abou-Ras D, Rudmann D, Kostorz G, Spiering S, Powalla M, Tiwari AN. Microstructural and chemical studies of interfaces between Cu(In,Ga)Se_2 and In_2S_3 layers. *Journal of Applied Physics* 2005; **97**(8): 084908-1-8. 10.1063/1.1863454.
132. Abou-Ras D, Kostorz G, Strohm A, Schock HW, Tiwari AN. Interfacial layer formations between Cu(In, Ga)Se_2 and In_xS_y layers. *Journal of Applied Physics* 2005; **98**(12): 123512-1-7. 10.1063/1.2149166.
133. Allsop NA, Camus C, Hänsel A, Gledhill SE, Lauermann I, Lux-Steiner MC, Fischer CH. Indium sulfide buffer/CIGSSe interface engineering: improved cell performance by the addition of zinc sulfide. *Thin Solid Films* 2006; **515**(15): 6068–6072. 10.1016/j.tsf.2006.12.084.
134. Abou-Ras D, Kostorz G, Hariskos D, Menner R, Powalla M, Schorr S, Tiwari AN. Structural and chemical analyses of sputtered In_xS_y buffer layers in Cu(In,Ga)Se_2 thin-film solar cells. *Thin Solid Films* 2009; **517**(8): 2792–2798. DOI:10.1016/j.tsf.2008.10.138
135. Pistor P, Allsop N, Braun W, Caballero R, Camus C, Fischer CH, Gorgoi M, Grimm A, Johnson B, Kropp T, Lauermann I, Lehmann S, Mönig H, Schorr S, Weber A, Klenk R. Cu in In_2S_3: interdiffusion phenomena analysed by high kinetic energy X-ray photoelectron spectroscopy. *Physica Status Solidi (a)* 2009; **206**(5): 1059–1062; published on line DOI: 10.1002/pssa.200881162
136. Barreau N, Deudon C, Lafond A, Gall S, Kessler J. A study of bulk $Na_xCu_{1-x}In_5S_8$ and its impact on the Cu(In,Ga)Se_2/In_2S_3 interface on solar cells. *Solar Energy Materials & Solar Cells* 2006; **90**: 1840–1848. 10.1016/j.solmat.2005.11.008.
137. Guillot-Deudon C, Harel S, Mokrani A, Lafond A, Barreau N, Fernandez V, Kessler J. Electronic structure of $Na_xCu_{1-x}In_5S_8$ compounds: X-ray photoemission spectroscopy study and band structure calculations. *Physical Review B* 2008; **78**: 235201. 10.1103/PhysRevB.78.235201.
138. Barreau N, Gall S, Marsillac S, Kessler J, Rockett A. The influence of copper and sodium diffusion across the CIGSe/In_2S_3 interface on solar cell properties. *Proceedings of the 20th European Photovoltaic Solar Energy Conference*, Barcelona, 2005; 1717–1721.
139. Jacob F, Barreau N, Gall S, Kessler J. Performance of $CuIn_{1-x}Ga_xSe_2$/(PVD)In_2S_3 solar cells versus gallium content. *Thin Solid Films* 2007; **515**: 6028–6031. 10.1016/j.tsf.2006.12.052.
140. Strohm A, Schlötzer T, Nguyen Q, Orgassa K, Wiesner H, Schock HW. New approaches for the fabrication of Cd-free CIGSe heterojunctions. *Proceedings of the 19th European Photovoltaic Solar Energy Conference*, Paris, 2004; 1741–1744.
141. Barreau N. Indium sulfide and relatives in the world of photovoltaics. *Solar Energy* 2009; **83**: 363–371. 10.1016/j.solener.2008.08.008.
142. Nakada T, Yagioka T, Yasaki Y, Mise T. Cd-free flexible CIGS thin film solar cells. *23rd European Photovoltaic Solar Energy Conference*, 2008; 2175–2178.
143. Kushiya K, Kuriyagawa S, Hara I, Nagoya Y, Tachiyuki M, Fujiwaara Y. Progress in large-area

CIGS-based modules with sputtered-GZO window. *Proceedings of the 29th IEEE Photovoltaic Specialists Conference*, 2002; 579–582.
144. Terada N, Kashiwabara H, Teshima S, Okuda T, Obara K, Yagioka T, Nakada T. Study of band alignment at CBD-Zn(S,O,OH)/CIGS interface by PES/IPES. *Technical Digest of 17th International Photovoltaic Science and Engineering Conference*, 2007; 205–208.
145. Naghavi N, Hubert C, Darga A, Renou G, Ruiz CM, Etcheberry A, Hariskos D, Powalla M, Guillemoles JF, Lincot D. On a better understanding of the post-treatment effects on the CI(G)S/Zn(S,O,OH)/ZnMgO based solar cells. *Proceedings of the 23rd European Photovoltaic Solar Energy Conference*, 2008; 2160–2164.
146. Minemoto T, Hashimoto Y, Satoh T, Negami T, Takakura H. Variable light soaking effect of Cu(In,-Ga)Se_2 solar cells with conduction band offset control of window/Cu(In,Ga)Se_2 layers. *Proceedings of the Materials Research Society Symposium*, San Francisco, 2007; 271–276.
147. Zabierowski P, Platzer-Björkman C. Influence of metastabilities on the efficiency of CIGSe-based solar cells with CdS, Zn(O,S) and (Zn,Mg)O buffers. *Proceedings of the 22nd European Photovoltaic Solar Energy Conference*, Milano, 2007; 2395–2400.